Rare Met. (2024) 43(6):2444–2468
https://doi.org/10.1007/s12598-023-02586-5

RARE METALS

REVIEW

Recent progress of Pt-based oxygen reduction reaction catalysts for proton exchange membrane fuel cells

Feng Zhan, Kun-Song Hu, Jin-Hua Mai, Li-Sheng Zhang, Zhen-Guo Zhang*, Huan He*, Xin-Hua Liu*

Received: 21 March 2023 / Revised: 25 April 2023 / Accepted: 4 May 2023 / Published online: 29 February 2024

Abstract With the increasing consumption of fossil fuels, proton exchange membrane fuel cells (PEMFCs) have attracted considerable attention as green and sustainable energy conversion devices. The slow kinetics of the cathodic oxygen reduction reaction (ORR) has a major impact on the performance of PEMFCs, and although platinum (Pt) can accelerate the reaction rate of the ORR, the scarcity and high cost of Pt resources still limit the development of PEMFCs. Therefore, the development of low-cost high-performance ORR catalysts is essential for the commercial application and development of PEMFCs. This paper reviews the research progress of researchers on Pt-based ORR catalysts in recent years, including Pt/C catalysts, Pt-based alloy catalysts, Pt-based intermetallic compounds, and Pt-based single-atom catalysts (SACs), with a focus on Pt-based alloy catalysts with different nanostructures. We described in detail the difficulties and solutions in the research process of various ORR catalysts and explained the principle of their activity enhancement with density functional theory (DFT). In addition, an outlook on the development of Pt-based catalysts is given, and reducing the amount of Pt used and improving the performance of catalysts are the directions to work on in the coming period.

Keywords Pt-based catalysts; PEMFCs; Pt-based intermetallic compounds; Single-atom catalysts

1 Introduction

There is an urgent need to develop green and sustainable energy and energy conversion devices due to the growing energy shortage caused by the accelerated consumption of conventional fossil energy and the resulting climate problems [1–3]. Pure, sustainable, and inexpensive hydrogen energy and its energy conversion device, the hydrogen fuel cell, have naturally attracted a lot of attention [4–6]. Proton exchange membrane fuel cells (PEMFCs) have great potential to solve energy and climate problems because they offer the advantages of high power density, superior energy conversion efficiency, low operating temperature, fast start-up, excellent stability, and environmental friendliness [7–10].

The catalyst is one of the core materials of PEMFCs and has a significant impact on fuel cell production costs, energy conversion efficiency, and battery life [11]. However, the sluggish kinetics of oxygen reduction reaction (ORR) is a major limitation for the further development of PEMFCs [12], so the development of ORR catalysts with high catalytic activity and high stability is essential [13, 14]. The ORR catalysts currently in widespread use are mainly Pt-based catalysts, non-precious metal catalysts,

F. Zhan, K.-S. Hu, J.-H. Mai, H. He*
School of Resources, Environment and Materials, Guangxi University, Nanning 530004, China
e-mail: noblehe@gxu.edu.cn

L.-S. Zhang, X.-H. Liu*
School of Transportation Science and Engineering, Beihang University, Beijing 102206, China
e-mail: liuxinhua19@buaa.edu.cn

Z.-G. Zhang*
IDTECH (Suzhou) Co. Ltd, Suzhou 215217, China
e-mail: zhenguo.zhang@idtechgroup.cn

X.-H. Liu
Dyson School of Design Engineering, Imperial College London, London SW7 2AZ, UK

and non-metallic catalysts [15, 16]. Pt-based catalysts refer to catalysts with Pt or Pt alloys as active components, which have the advantages of high activity, strong anti-poisoning ability, and highly efficient reactions at low temperature, low pressure, and a wide pH range [17]. Non-precious metals are widely used in catalysts due to their relatively low prices and rich valence states. The application of oxygen reduction catalysts mainly focuses on the transition metals Fe, Mn, Co, Cu, Ni, Zn, etc. The main types are transition metal oxides, transition metal carbides, transition metal nitrides, and metal-nitrogen-doped carbon materials (M-N-C, M = Fe, Co, Ni, Mn, etc.) [18]. Among these, M-N-C has relatively good catalytic activity and stability in alkaline and acidic electrolytes and is considered the most likely catalyst to replace platinum [19]. However, it also faces problems such as metal leaching, the combination of anions and active sites, and the protonation of doped nitrogen in acidic environments [20]. Non-metallic catalysts refer to a heteroatom-doped sp^2 hybrid carbon-based materials. The inherent porosity, porous structure, and electrical conductivity of carbon materials are extremely advantageous for the production of highly active catalytic materials [21]. However, it lacks sufficient active sites, so heteroatoms (such as B, N, P, S) are often introduced to improve its interaction with adsorbed species and promote the reaction [22]. As the adsorption and dissociation mechanisms of O_2 on the surface of Pt are relatively simple, the most efficient catalysts for ORR are still Pt-based [23]. However, the scarcity and high cost of Pt resources limit the long-term development of PEMFCs, so current researches are focused on reducing the use of Pt while improving its catalytic activity [24, 25].

This paper reviews recent research progress in the preparation and modification of Pt-based catalysts (including Pt/C catalysts, Pt-based alloy catalysts [26], Pt-based intermetallic compound catalysts [27], and Pt-based single-atom catalysts (SACs) [28]) for ORR, starting from the improvement of catalyst activity and durability. The preparation and performance enhancement methods of the above four types of catalysts are discussed in detail in separate chapters, focusing on the methods for improving the overall performance of catalysts by modifying the nanostructure of Pt-based alloy catalysts. Finally, this paper also provides an outlook on the development of Pt-based catalysts, as the development of high-activity, low-cost, and sustainable catalysts is the main direction for the development of ORR catalysts in the future.

2 Pt/C catalyst

In the early stages of fuel cell development, only Pt nanoparticles (NPs) were used for the ORR, but without support, Pt NPs tended to agglomerate and seriously affect catalytic performance, which could not meet practical requirements [29]. And then, the researchers found that using conductive carbon to support the Pt NPs could reduce the amount of Pt used and prevent agglomeration of the Pt NPs [30]. This chapter mainly describes recent efforts of researchers to improve the activity of Pt/C catalysts and reduce the amount of Pt used. Supporting Pt on carbon can effectively reduce the amount of Pt, but the Pt must be uniformly distributed on the carbon support for the catalyst to have excellent performance. The addition of surfactants during the preparation of catalysts is a common means of improving their dispersion, as surfactants can sterically confine Pt. It is also a good way to improve the dispersion of catalysts that using novel mesoporous carbons as supports. In addition to improving dispersion, it is critical to address the corrosion of carbon supports when using Pt/C catalysts. It has been found that in addition to using some carbon supports with corrosion resistance (such as graphene, carbon nanotubes (CNTs), and carbon nanofibers), other elements can be doped into the carbon supports, which enhance the electronic metal-support interaction (EMSI) and anchor Pt on the supports. Coating the outer layer of Pt with a thin layer of carbon can not only improve the dispersion of Pt, but more importantly, it can prevent direct contact between Pt and the electrolyte during use. This can inhibit the adsorption of toxic substances on the catalyst, improving the stability of the catalyst and increasing its anti-poisoning ability. Corrosion resistance and electrical conductivity can be combined when other corrosion-resistant supports and carbon supports are prepared into a composite support, and when this composite support is used to support Pt, the stability of the catalyst can be improved.

Highly dispersed catalysts are known to expose more efficient active sites and considerably increase Pt utilization, allowing catalysts to exhibit superior catalytic activity [31, 32]. Researches have shown that the addition of tensides during the preparation process may result in steric confinement of Pt to improve the dispersion of Pt on the support [33, 34]. For example, Sun et al. [35] used polyvinylpyrrolidone (PVP) as a surfactant to prepare high-loading (> 40 wt%) Pt/C catalysts with ultrafine particle size ($\sim$ 3.19 nm) and good dispersion using microwave-assisted preparation. During the reaction, PVP not only spatially confines Pt but also rapidly decomposes, reduces, and carbonizes with Pt precursors to form Pt@C structure supported on carbon black. The thin carbon layer on the Pt outer layer in this structure can not only suppress the agglomeration of Pt NPs but also prevent the poisoning of the Pt core, thus improving the activity and durability of the catalyst. Ruiz-Camacho et al. [36] investigated the effect of loading different supports, such as graphene oxide

(GO), reduced graphene oxide (rGO), carbon Vulcan (XC72R), and Go–C (1:1) on the catalysts. And they found that the oxygen functional groups on the GO surface could promote the uniform distribution of Pt NPs, resulting in the highest dispersion among several catalysts. In addition, GO could modify the electronic properties of Pt, improving its catalytic activity. Carbon materials with a large surface area can also be selected as supports for Pt, improving the electrochemically active surface area (ECSA) of the catalyst, exposing additional active sites, and improving catalyst activity. Xie et al. [37] chose a new mesoporous carbon (3#) to compare with commercial graphitized carbon (C18) and porous carbon (EC300) as supports to investigate the effect of the supports' specific surface area on catalyst performance. The abundant mesoporous structure and large specific surface area of 3# provided a large number of sites for Pt deposition, resulting in Pt particles that are not only uniformly distributed on the surface of the carbon support but also in the mesoporous interior of the support. Finally, for the sample with 3# as support, the ECSA of 92 $m^2 \cdot g^{-1}$ was obtained, which was much higher than that of the other two groups of samples, which were 50 and 40 $m^2 \cdot g^{-1}$, respectively. This "internal Pt" structure constructs effective three-phase boundaries (TPB), which can avoid the toxic effect of the ionomer on the NPs, then reduce the activation impedance and the oxygen mass transfer impedance, and improve the reaction efficiency so that Pt/3# (150 $mA \cdot mg_{Pt}^{-1}$) has a much higher mass activity than the other two groups of samples (86 and 78 $mA \cdot mg_{Pt}^{-1}$).

The carbon support of Pt/C catalysts is easily corroded in practice, and the result is the agglomeration of Pt NPs, which has a seriously detrimental effect on the performance of the catalyst. Labata et al. [38] investigated the degradation mechanism of Pt/C catalysts during ORR in different pH media. Studies have found that in acidic electrolytes, catalysts would form oxides (mainly O–C=O functional groups) on the carbon surface after working at limiting potentials, leading to Pt poisoning and severe loss of ORR activity. Under alkaline conditions, after a steep potential cycle of the Pt/C catalyst, the higher mobility of Pt leads to an increase in aggregates and a decrease in ECSA due to the dissolution of the carbon layer. The durability of the catalyst can be effectively increased by strengthening the carbon support. For example, Bai et al. [39] ultrasonicated Pt/C and a certain amount of KBH_4 in deionized water for a certain time, then heated it at an elevated temperature, centrifuged it to remove impurities, and dried it to obtain a modified catalyst Pt/C-M (0.13, 180). X-ray photoelectron spectroscopy (XPS) characterization of the catalysts before and after modification showed that the content of O–C=O groups decreased slightly after modification, indicating that the O–C=O groups were reduced by KBH_4 (Fig. 1a). The reduction of oxygen-containing groups was observed in the O 1s spectrum (Fig. 1b), and the absolute content of O-Pt bonds in Pt/C-M (0.13, 180) was also found to be reduced. Combined with transmission electron microscopy (TEM) and electrochemical characterization, it was found that the method reduced the surface defects of Pt NPs by reducing the oxygen-containing functional groups on the surface of the carbon support, effectively alleviating the corrosion of carbon, and inhibiting the agglomeration and growth of Pt NPs. The mass activity (MA) and specific activity (SA) of the KBH_4-modified catalyst were 1.14 and 1.29 times higher, respectively, than those of the original sample (Fig. 1c). Moreover, after 10,000 cycles, the MA loss of the modified sample was only 6.26%, while that of the original sample is 16.52%, which significantly improves the stability. Park et al. [40] used Pickering emulsion to treat the Pt/C catalyst to improve catalyst stability. Observing TEM image (Fig. 1d) of the graphene-Pt/C composite before and after cycling, it can be seen that the graphene nanoplatelets mitigate the Pt loss during cycling by providing redeposition and localization sites for Pt NPs. As shown in the figure, there is a small number of Pt NPs on the graphene nanoplatelets after the initialization step (see the white arrow), and the size and number of Pt NPs on the graphene nanoplatelets continue to increase during 30,000 cycles. And they are preferentially formed on the edges of the graphene nanoplatelets rather than on the graphene basal surfaces. This suggests that the modified graphene nanoplatelets provide anchoring sites for Pt nanoparticle redeposition and suppress Pt loss during cycling. This allows the catalyst to retain a greater proportion of the active surface area after long-term cycling, with an ECSA loss of only 25.1% after 30,000 cycles compared to 36.3% for untreated Pt/C (Fig. 1e). In addition, the graphene-Pt/C composite provides an open microstructure with minimal barriers to reactant entry and product exit from the catalytic active site, resulting in superior initial ECSA and ORR activity.

It has been shown that when Pt is loaded with materials such as graphene [41], CNTs [42–44], and carbon nanofibers [45], the catalysts have good corrosion resistance. The use of other elements to dope these carbon materials for Pt loading not only makes the support more resistant to corrosion but also creates a synergy with Pt to improve the activity and stability of the catalyst [46–52]. Choi et al. [53] used density functional theory (DFT) to investigate the reason for the improved catalyst performance when graphene was used as a support and found that the catalyst had high activity and stability due to the strong Pt-C covalent bond and the unique surface morphology of Pt and graphene. Carbon atoms in graphene form covalent bonds with

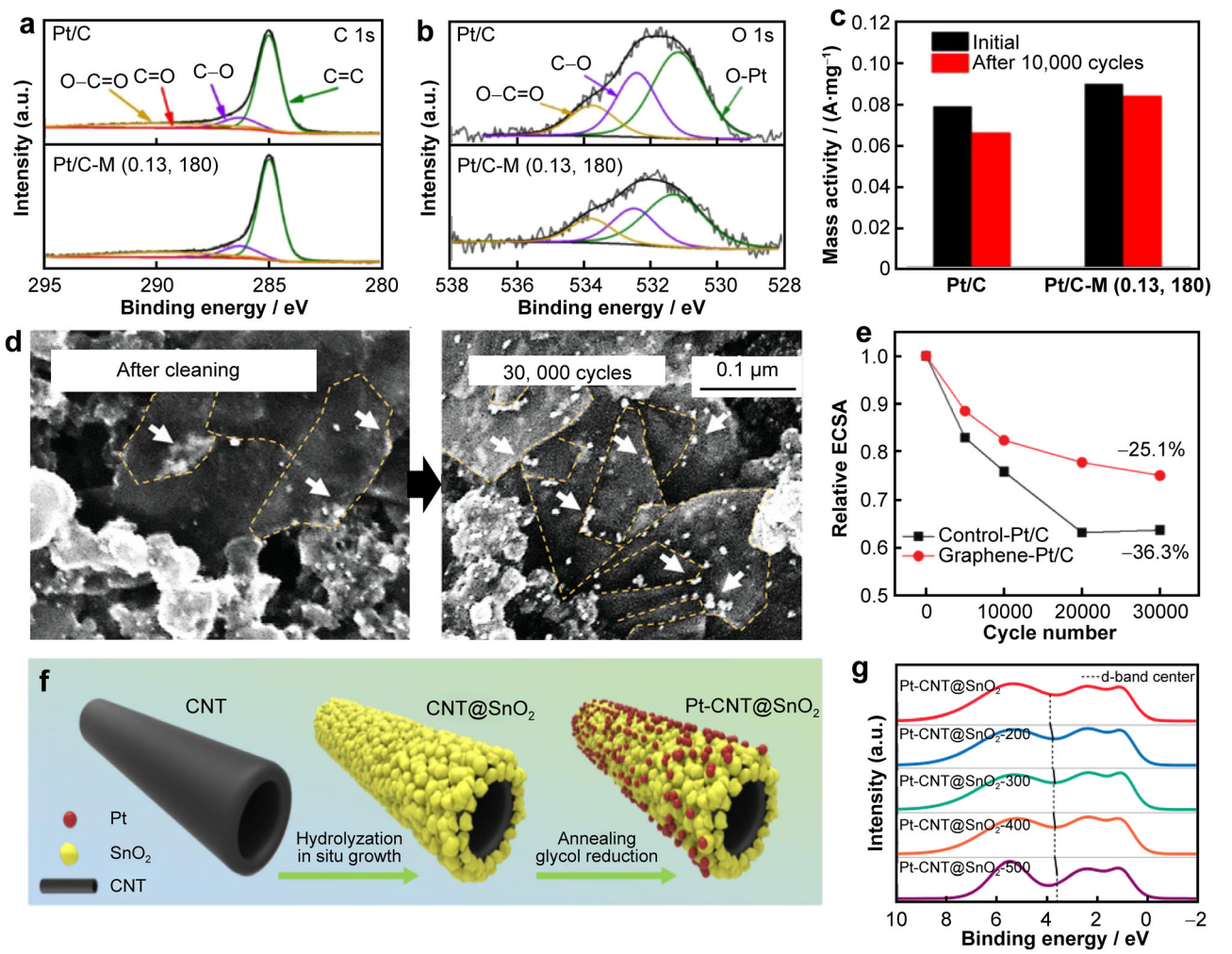

Fig. 1 High-resolution XPS spectra of **a** C 1s and **b** O 1s before and after KBH_4 modification of catalyst; **c** summary of MA of Pt/C and Pt/C-M (0.13, 180) before and after 10,000 cycles of accelerated durability tests (ADTs). Reproduced with permission from Ref. [39]. Copyright 2022, American Chemical Society. **d** SEM images of graphene-Pt/C composites before and after cycling; **e** plot of ECSA versus number of turns obtained for catalysts cycled to 30,000 turns before and after Pickering emulsion treatment at between 0.60 and 0.95 V (vs. RHE). Reproduced with permission from Ref. [40]. Copyright 2022, John Wiley and Sons. **f** Pt-CNT@SnO_2-T synthetic route schematic diagram; **g** valence band XPS spectrum of Pt-CNT@SnO_2-T, where black dashed line indicates location of d-band center. Reproduced with permission from Ref. [59]. Copyright 2022, Elsevier

Pt atoms to produce an alternating sp^2-sp^3 hybridization wave surface morphology. The sp^2 region of graphene provides active sites for ORR, and all active sites on the Pt surface are provided by Pt-C (sp^3). Moreover, the ORR on the graphene surface is easier to perform due to the weaker oxygen-binding energy and lower excess potential than that on Pt surface. Nechiyil et al. [54] proposed a method for nitrogen-sulfur co-doped carbon nanotubes (NS-PECNTs) to improve the interface bonding between the support and the catalyst NPs. Studies have shown that there is a strong interaction between Pt NPs and dopants or defect sites, which can anchor Pt and play a crucial role in improving ORR activity, fuel cell performance, and catalyst durability.

Forming a carbon coating on the surface of the Pt to prevent direct contact between the Pt and the electrolyte is also a method of improving the durability of the catalyst. Chen et al. [55] used DFT to cover two-dimensional graphene (GDY) with uniformly distributed pores on the Pt surface for catalytic ORR. They found that Pt would form a GDY/Pt(111) heterophase interface with GDY and that GDY on the surface would weaken the adsorption of CO by Pt(111) and inhibit CO poisoning of the catalyst. These were the main reasons for the improved stability and activity of the catalyst. Liu et al. [56] soaked and adsorbed polydopamine on commercial Pt/C to form a coating on Pt grains, and then converted the coating to lesser-layer nitrogen-doped graphene by calcination to produce Pt/C@NC. It was found that the coating could effectively

block the direct contact between Pt NPs and electrolytes, avoid Ostwald ripening, inhibit the adsorption of toxic substances, improve the stability of the catalyst, and enhance the resistance to poisoning. More importantly, smearing does not affect the ORR activity of commercially available Pt/C.

The durability of the catalyst can be significantly improved by using the composite materials of carbon and other corrosion-resistant materials as a carrier. For example, Park et al. [57] used a simple hydrothermal method to prepare NG-TiON composites consisting of nitrogen-doped graphene and nitrogen-doped TiO_2 as supports for Pt/NG-TiON catalysts. It was found that the improved conductivity of the support resulting from the N doping of TiO_2 and further hybridization with N-doped graphene were the main reasons for the improved catalytic performance of Pt/NG-TiON. Furthermore, in a single-cell test of 5000 cycles, the degradation rate of the Pt/NG-TiON catalyst was only 9%, while the degradation rate of Pt/C was 83%, demonstrating that the NG-TiON material has an excellent corrosion resistance when used as a support. Xu et al. [58] developed a high corrosion resistance and an excellent electrical conductivity MXene ($Ti_3C_2T_x$) hybrid with CNT composite material as a support for Pt. The MA of the Pt/CNT-MXene catalyst was 3.4 times higher than that of the Pt/C catalyst due to the synergistic interaction between Pt and CNT-$Ti_3C_2T_x$. The ECSA of the Pt/CNT-$Ti_3C_2T_x$ (1:1) catalyst decreased by only 6% after the 2000 cycle potential sweeping, while that of Pt/C decreased by 27%. Li et al. [59] designed a cable-like core@shell CNTs@SnO_2 material with a regulable EMSI support for Pt. The structure and synthetic route of this material are shown in Fig. 1f. The valence band XPS spectra characterization of Pt-CNT@SnO_2 samples with different annealing temperatures (Fig. 1g) show that the d-band center of Pt shifts negatively with decreasing annealing temperature. This is because the large difference in work functions between Pt and SnO_2 enhances the charge transfer between them and fills the d-band of Pt with additional electrons, resulting in a negative shift of the d-band center of Pt and enhancing the intrinsic activity of the catalyst. At the same time, SnO_2 can act as a protective layer for CNTs and stabilize Pt NPs under PEMFC operating conditions. The ECSA loss of Pt-CNTs@SnO_2-400 is only 11.3% after 50,000 cycles, while the MA loss is only 9.2% after 5000 cycles, and the strong metal-support bonding interaction (SMSBI) endows Pt atoms with greater adhesion energy and migration barriers, giving the fuel cell very high stability.

Although Pt/C catalysts already have excellent catalytic activity and relatively mature processes following research and modification by a large number of researchers, there are still some problems that need to be addressed, such as dissolution and agglomeration of Pt particles, Ostwald ripening, and corrosion of the support [60–67]. To address these issues, in addition to improving the process for preparing finer and more homogeneous Pt nanoparticle catalysts, researchers have enhanced the EMSI by treating carbon supports so that Pt can be stably anchored to the supports. The doping of N, P and S into graphene, CNTs and carbon nanofibers can have a favorable anchoring effect on Pt. The carbon support can also be pre-treated so that its surface is rich in oxidation functional groups before support, and then Pt can be adequately dispersed on the support during support. The main obstacle to the commercialization of Pt/C catalysts is likely to be the scarcity of Pt resources and their high cost, which makes it difficult to achieve mass production. Therefore, it is particularly important to reduce the amount of Pt used as much as possible while improving the catalyst performance, and alloying Pt with other metals to produce Pt-based alloy catalysts is expected to solve this problem.

3 Pt-based alloy catalyst

Pt/C catalysts have excellent ORR activity, but the high cost and scarcity of Pt limit their wide application [68, 69]. Reducing costs and improving activity have become key tasks for Pt-based catalysts on commercial roads [70]. Alloying Pt with non-noble metal elements such as Co [71–74], Ni [75, 76], Cu [77], Fe [78], Sr [79], Gd [80], and Mg [81] not only significantly reduces the amount of Pt used but also improves catalyst activity. The addition of other elements can not only significantly reduce the amount of Pt used, but also create ligand and strain effects to optimize the surface electronic structure of Pt [82, 83]. This reduces the adsorption of oxygen-containing species on Pt during the ORR process, accelerating the rate-determining step (RDS) and increasing the intrinsic activity of the catalyst [84–86]. And some researchers, inspired by the concept of high-entropy alloys (HEAs), have demonstrated theoretically and experimentally that HEAs composed of multiple elements are beneficial for accelerating the ORR process [87–89]. Owing to the high entropy, lattice distortion, and sluggish diffusion effects of HEAs, Pt-based HEA nanocatalysts exhibit outstanding catalytic activity and stability for ORR [90]. To further improve the utilization rate of Pt and its catalytic activity, crystal orientation engineering and near-surface alloying are often used to adjust the surface activity of the catalyst [91–93]. Recently, researchers have discovered that Pt-based alloy catalysts and single-atom catalysts can be prepared as hybrid electrocatalysts. The synergistic effect between them can be used to increase the number of active sites and reduce the formation of H_2O_2. This reduces membrane and

ionomer degradation and improves catalyst activity and durability [94]. To address the Ostwald ripening, migration, and agglomeration of alloy catalysts during the cycle, researchers have attempted to modify the surface of Pt-based alloys using surfactants to suppress the formation of Pt oxide layers and enhance the durability of the catalysts [93, 95]. Not only can specific nanostructures provide additional specific surface areas and higher active sites [96], but they can also increase effective electron transfer pathways and reduce interfacial resistances [97]. The preparation of Pt alloys into special nanostructures not only enhances the ligand and electronic effect but also exposes additional active sites, which further increases catalytic activity [98]. In this chapter, the preparation of different nanostructures of Pt-based alloy catalysts and the performance enhancement methods are described in three subchapters, and different nanostructures have different effects on the catalyst's performance. The unique one-dimensional (1D) nanostructure not only reduces the activation energy but also significantly weakens the interaction between Pt and oxygen-containing species. All these can lead to a significant improvement in reaction kinetics. Polyhedral nanostructures can expose more highly efficient crystal faces and have an excellent stability. When nanopolyhedra are made as hollow structures, it not only leads to a further reduction in Pt usage, but also enables the creation of additional reaction sites and shorter charge transfer distances. This accelerates the sluggish kinetics of the ORR.

3.1 1D nanostructures

1D nanostructures usually have high aspect ratios, which endow advanced electron transfer capabilities. The channels or gaps between 1D structures provided by nanotubes can speed up reaction kinetics by accelerating the transport of reactant and product [99, 100]. This section mainly describes how to improve the activity and stability of catalysts by improving the 1D nanostructure of Pt-based alloys. The 1D nanostructures give excellent catalyst activity and stability due to their unique structure, but they still have some problems such as dissolution of alloying elements. Researchers have conducted extensive studies to address this challenge. It was found that catalysts could be prepared in heterogeneous 1D structures to reduce their surface energy, while doping with additional elements could tune the electronic structure and improve the stability of the catalyst, thus maintaining its high activity. Making the catalysts into ultra-thin nanorods and nanotubes not only improves the stability of the catalysts but also significantly increases the utilization of Pt.

1D nanostructures with intrinsic anisotropy and multiple carbon binding sites enhance EMSI, reduce Pt migration, and effectively suppress Ostwald ripening and agglomeration [101]. Lei et al. [102] used a simple elevated temperature solid-phase method to synthesize Pt-M (M = Fe, Co, and Ni) bimetallic nano-branched structure (NBs) catalysts. The SA and MA of Pt-M NBs are 6.1 and 5.3 times higher than those of commercial Pt/C samples, respectively, due to the kink structures and abundant ladder on the surfaces. The loss of SA and MA of the Pt-M NBs catalysts after 10,000 accelerated durability tests (ADTs) was only 4.0% and 14.4%, respectively. Cao et al. [103] synthesized compositionally controllable PtCu porous nanowires (PNWs) by an ultrasound-assisted galvanic replacement reaction. TEM characterization revealed that PtCu PNWs were composed of many small NPs with random orientations, which were interconnected to form nanopores. This open structure can facilitate proton/mass transfer during ORR, provide abundant defect sites, and increase the surface area-to-volume ratio. Observation of the high-resolution TEM (HRTEM) images and X-ray diffraction (XRD) characterization shows that Cu atoms in PtCu PNWs can cause significant lattice contraction. Using XPS analysis, it is found that Pt in PtCu PNW is mainly in the zero-valence state, which can provide more active sites, and thus improve catalytic performance. In addition, electronic interactions between Pt and Cu atoms in PtCu PNWs were found. Pt atoms with a higher electronegativity can accept electrons from Cu atoms, resulting in a downward shift of the d-band center relative to the Fermi level. Therefore, the formation of PtCu alloy can reduce the oxygen affinity and release more active sites, thereby increasing the catalytic efficiency of ORR. Under the synergistic effects of 1D structure, strain effect, electronic effect, and alloy effect, the prepared $Pt_{0.5}Cu_{0.5}$ PNWs catalyst had excellent catalytic activity. The $Pt_{0.5}Cu_{0.5}$ PNWs had a mass activity of 800 $mA{\cdot}mg_{Pt}^{-1}$ and specific activity of 1.52 $mA{\cdot}cm_{Pt}^{-2}$, both higher than the JM Pt/C catalyst (160 $mA{\cdot}mg_{Pt}^{-1}$, 0.22 $mA{\cdot}cm_{Pt}^{-2}$). Due to the 1D structure and stable porous structure, even after 10,000 cycles of the accelerated durability test, the MA degradation of the $Pt_{0.5}Cu_{0.5}$ PNWs catalyst was only 8.4%, which was much lower than that of the JM Pt/C (43.7%).

Several researchers have improved the stability of catalysts through the preparation of 1D nanostructures with unconventional morphologies. For example, Li et al. [104] incorporated Ga into Pt_3Co nanowires to prepare a lavender-structured Ga-Pt_3Co/C catalyst consisting of PtGa stems and PtCoGa surface leaves, whose TEM and structural schematic are shown in Fig. 2a. They investigated the effect of Ga doping on the stability of the catalyst by calculating the surface energies of pure Pt, Pt_3Co and Ga-Pt_3Co (111) surfaces, the results of which are shown in Fig. 2b. It can be seen from this figure that the surface

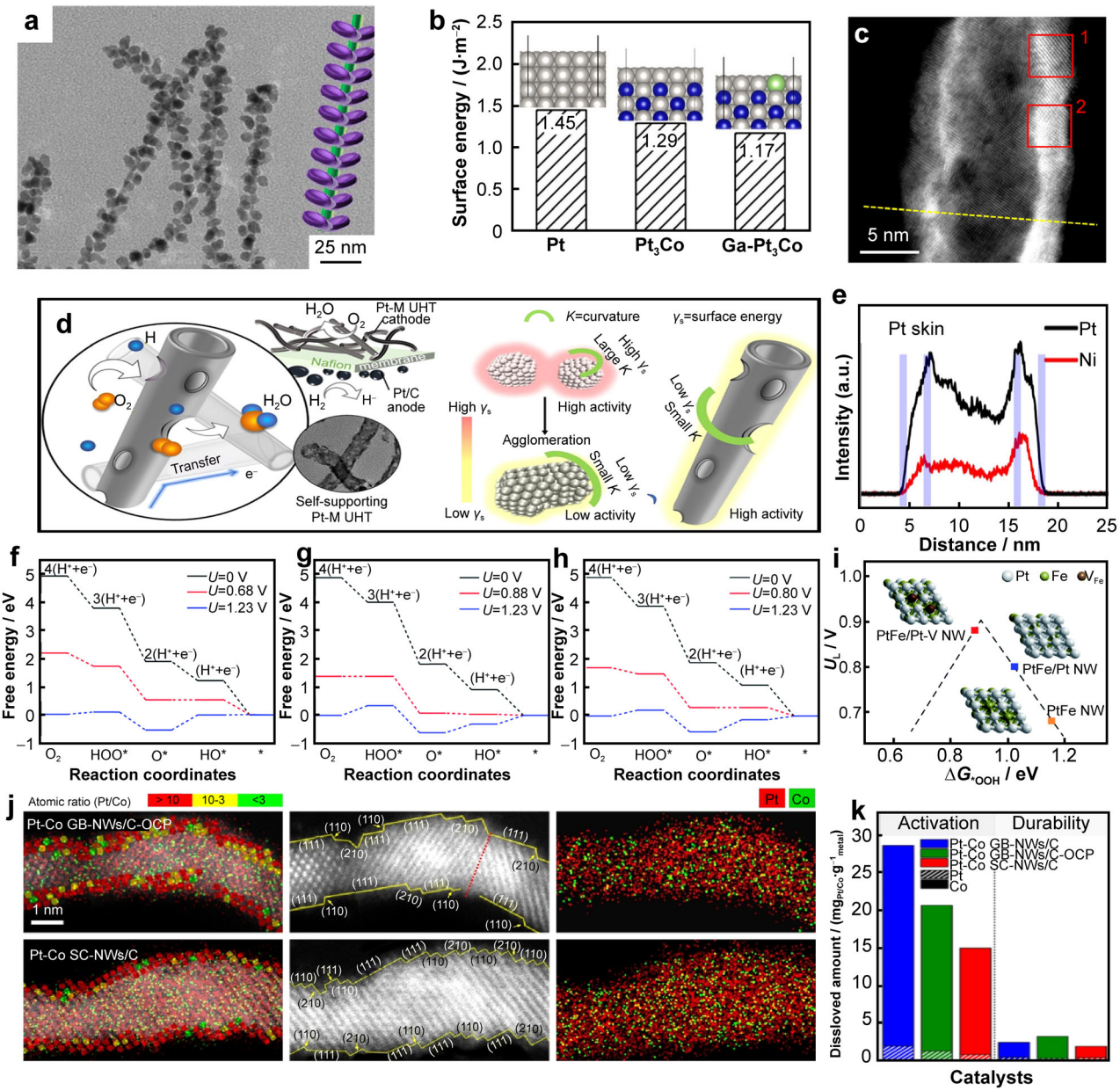

Fig. 2 **a** TEM image of Ga-Pt_3Co and (inset) schematic illustration of its structure; **b** surface energy of pure Pt, Pt_3Co and Ga-doped Pt_3Co (111) surfaces. Reproduced with permission from Ref. [104]. Copyright 2020, American Chemical Society. **c** HAADF-STEM image of Pt-Ni UHT; **d** schematic diagram of ORR catalytic layer of UHT for PEMFCs; **e** FFT results of Pt-Ni UHT. Reproduced with permission from Ref. [108]. Copyright 2022, American Chemical Society. DFT calculation results for **f** PtFe NW, **g** PtFe/Pt-V NW, and **h** PtFe/Pt NW for adsorption energy of oxygen-based intermediates; **i** activity volcano curve of PtFe/Pt NW. Reproduced with permission from Ref. [109]. Copyright 2021, Royal Society of Chemistry. **J** HAADF-STEM and EDS images of Pt-Co GB-NWs/C-OCP and Pt-Co SC-NWs; **k** dissolved amounts of Pt and Co during activation and durability test of Pt-Co GB-NWs/C-OCP and Pt-Co SC-NWs/C, where dissolved amounts have been normalized to total metal loading. Reproduced with permission from Ref. [110]. Copyright 2022, American Chemical Society

energy of Ga-Pt_3Co (111) is significantly lower than that of the remaining two groups, indicating that Ga doping can significantly improve the stability of the Pt_3Co surface. Kong et al. [105] synthesized surfactant-free Pt-iron alloy twisty nanowire catalysts (Pt-Fe TNWs) with twisted and helical shapes in a hydrothermal kettle using N, N-dimethylformamide (DMF) as the solvent. It was found that the special alloy structure and significant lattice strain in Pt-Fe TNWs gave the catalyst excellent activity and durability (MA was about 20 times higher than that of commercial Pt/C catalysts, and $< 2\%$ loss of activity after 40,000 cycles and $< 30\%$ loss after 120,000 cycles).

Some scientists also used elemental doping to improve the activity and durability of catalysts. Zhang et al. [106] synthesized S-doped AuPbPt alloy nanowire networks (NWNs) by conformal growth of Pt onto preformed S-doped AuPb NWNs in water at pH 2. Experimental and computational results show that a certain amount of PtS will be produced in the S-doped AuPbPt alloy NWNs, and an appropriate amount of PtS will reduce the d-band center of Pt, thereby making Pt have stronger ORR catalytic activity. This study provides a theoretical and practical basis for the doping of non-metallic elements into the Pt alloy lattice and offers new ideas for reducing the amount of Pt used, enhancing the activity and durability of Pt alloy catalysts. Deng et al. [107] prepared a Mo-doped Pt_3Co alloy nanowire (Pt_3Co-Mo NWs) with high-quality activity and specific activity. DFT calculations have shown that Mo doping can change the electronic structure of both Pt and Co. The addition of Mo not only optimizes the interfacial oxygen-binding energy but also increases the vacancy formation energy of Co. The rational integration of multiple advantages, such as alloy features, 1D nanowires, and high-index facets, in composition and structure endows Pt_3Co-Mo NWs with good durability, with a retention rate of 76% after 50,000 potential cycles. Some researchers have also made Pt-based alloys into ultra-thin nanotubes to improve the use of Pt and increase the stability of catalysts during use. For example, Liu et al. [108] prepared Pt-M (M = Ni, Co) ultrathin holey nanotube (UHT) catalysts by electrostatic spinning and heat treatment and used them in the ORR catalytic layer of PEMFCs, the principle of action of which is shown in Fig. 2d. The high-angle annular dark-field scanning transmission electron microscopy (HAADF-STEM) image showed that the Pt-Ni UHT had a diameter of about 15 nm, rough and holey tube walls, and an ultrathin wall thickness of about 2–3 nm (Fig. 2c). They also demonstrated that Ni successfully entered the Pt lattice using fast Fourier transformation (FFT) (Fig. 2e). Electrochemical tests found that Pt-M UHT had a smaller ECSA than Pt/C, but higher MA and power density, which meant that the intrinsic activity of Pt-M UHT was higher than that of Pt NPs. This is due to the combined effect of the high utilization of Pt atoms resulting from the efficient mass transfer and 100% surface exposure of the nanotube structure combined with the alloying effect. Furthermore, the nanotube structure not only avoids the problem of nanoparticle agglomeration, but the low curvature of the tube wall also gives the UHT a low surface energy, making it more resistant to Oswald ripening and more stable.

We all know that defects in materials have a profound effect on their performance, and the same is true of catalysts. For example, Shi et al. [109] prepared PtFe/Pt-V NW nanowire catalysts with abundant surface vacancies by electrochemical de-alloying, which had excellent activity and durability. They then used DFT calculations to explore the principle of surface vacancies improving the activity, and the results are shown in Fig. 2f-h. From these figures, it can be seen that for PtFe/Pt-V NWs with abundant Fe vacancies on the surface, the RDS of ORR is the formation of OOH^*, while for the electrocatalyst without vacancies on the surface, the RDS is the formation of OH^*. The activity volcano diagram of the free energy barrier forming $^*OOH$ (ΔG^*_{OOH}) descriptor is shown in Fig. 2i. The activity of PtFe/Pt-V NW is near the top of the volcano plot, indicating that it has the best ORR activity among these catalysts. Overall, the vacancies present on the catalyst surface can weaken the binding and adsorption of Pt to oxygen-containing intermediates, alter the RDS of the ORR process, and thus increase the ORR activity. However, another kind of defect in the crystal structure—the grain boundaries (GBs)—has a hindering effect on the ORR process. To understand the principles, Kabiraz et al. [110] prepared Pt-Co GB-NWs/C-OCP and Pt-Co SC-NWs/C for comparison, which had very similar diameters, Pt-Co ratios, and Pt-rich surface structures, except for the GBs. Figure 2j shows the HAADF-STEM and energy-dispersive X-ray spectroscopy (EDS) characterization of Pt-Co GB-NWs/C-OCP and Pt-Co SC-NWs/C. It can be seen that the surface composition and structure of the two samples are relatively close to each other. During the study, it was found that the presence of GBs in Pt-Co NWs promoted the leaching of Co (Fig. 2k). Finally, it is concluded that the surface GB sites are deactivated by causing element leaching and may not act as ORR promoters for Pt-Co nanowire catalysts.

3.2 Polyhedral nanostructures

The preparation of Pt-based alloy catalysts into polyhedrons is also an important means of improving their performance [111]. However, Pt alloys with a simple octahedral structure often have the problem of non-noble metal elements dissolving, causing the polyhedron to collapse and affecting the activity and durability of the catalyst [112]. This subsection focuses on some of the methods used to improve the stability of the polyhedral structure while improving catalyst activity and durability. The formation of a thin layer of Pt on the surface of the polyhedron, the doping of the polyhedron with other elements, the preparation of polyhedrons with heteromorphic structures, etc., can all play a certain role in improving the stability and activity of polyhedron catalysts.

The formation of a thin Pt layer on the surface of the polyhedral structure not only shortens the reaction path and increases the catalytic activity, but also protects the internal

structure and improves the stability of the catalyst. Kong et al. [113] prepared octahedral $Pt_{1.5}Ni$ nanocatalysts by a thermal reduction method. Subsequently, the surface/near-surface structure of the octahedron was atomically regulated by heat treatment, pickling, etc., and an octahedral PtNi alloy catalyst (A-MS-$Pt_{1.5}$Ni) with an extremely thin Pt-rich shell was obtained. The schematic diagram of its synthesis is shown in Fig. 3a. The HRTEM and HAADF-STEM-EDS images show a complete octahedral morphology. The surface of the octahedral structure mainly exposes the Pt (111) plane, providing favorable conditions for high activity. And A-MS-$Pt_{1.5}$Ni has Pt-rich layers on the outside and a Pt-Ni alloy structure on the inside. These Pt-rich layers can not only provide more active sites for ORR, but also protect the inner alloy structure. The inner Pt-Ni alloy structure can support the outer platinum-rich shell. The combination of XRD and XPS analysis showed that Ni in the alloy has modified the electronic structure of Pt. This is because the diffused Ni atoms have a lower electronegativity than Pt, causing the d-band center of Pt to exhibit a marked negative shift after alloying. The electrochemical characterization showed that its SA and MA were about 20 and 10 times higher, respectively, than the commercial sample Pt/C, as shown in Fig. 3b, c. To understand the mechanism behind this, the electronic density of states and the OH^* binding energy of the (111) crystal plane of the catalysts with different structures were calculated (Fig. 3d). The results show a significant negative shift in the d-band center of the optimized octahedral catalyst. The downward shift in the d-band center reduces the rate-determining step in the ORR reaction and therefore significantly improves the ORR activity. Xie et al. [114] additionally fabricated octahedral nanocrystals catalysts with ultrathin Pt layers and a schematic illustration of their synthesis is shown in Fig. 3e. Figure 3f shows ADTs results of the catalyst, which shows that the catalyst has a MA of 2.82 $A{\cdot}mg^{-1}$ and a SA of 9.16 $mA{\cdot}cm^{-2}$, which are 13.4 and 29.5 times higher than those of commercial Pt/C catalysts, respectively. Compared with the recent work of other researchers, it still has great advantages, as shown in Table 1. After 30,000 ADTs, the MA of the catalyst reduced by only 21%. The studies showed that growing alloy nanocluster structures on the polyhedral epidermis can prevent cluster aggregation and loss of active sites near the surface and have higher stability and more active sites. For example, Zhao et al. [115] prepared the Pt-rich PtCu heteroatom clusters epitaxially grown on the octahedral PtCu alloy/Pt skin matrix ($PtCu_{1.60}$). Owing to the synergy of electronic effects, abundant low-coordination sites, and compressive strain, $PtCu_{1.60}$/C has a $4e^-$ ORR pathway and a MA 8.9 times higher than that of commercial Pt. There was almost no decrease in activity after the 140,000 cycles. DFT calculations show that Pt-rich and PtCu clusters improve ORR activity and thermodynamic stability, resulting in a greater catalyst life.

Some researchers doped polyhedra with other elements to improve the performance of the catalyst. Zhu et al. [116] successfully prepared Ru-doped Pt-Co octahedral catalysts (Ru-Pt_3Co/C), which have much higher ORR activity and stability than Pt_3Co/C and Pt/C. The in-site X-ray absorption fine structure (XAFS) result shows that Ru can drive the reduced Pt atoms back to their initial state after ORR by transferring redundant electrons from Pt to Ru, preventing the over-reduction of Pt active sites and improving chemical stability. DFT calculations show that Ru doping can accelerate the destruction and desorption of oxygen intermediates, thereby improving catalytic performance. And, Polani et al. [117] prepared Mo-doped Pt-Ni alloy octahedral catalysts with higher activity and durability, which further confirmed that doping polyhedra with other elements can significantly improve the activity and durability of catalysts.

Recently, researchers have found that the heteromorphic polyhedron will expose more active sites and have a larger ECSA, which improves the activity of the catalyst. Xia et al. [118] prepared unique Pt-Ni alloy polyhedral nanochains (Pt-Ni PNCs) by a one-pot method, and the HAADF-STEM image is shown in Fig. 3g. As we can see from the diagram, the polyhedral nanochain consists of ultrafine nanowires that connect neighboring nanopolyhedra. This ordered arrangement preserves the original structural advantage of each component while creating new interface relationships that help stimulate architectural synergies between the 0D and 1D nanostructures. In addition to the typical abundance of angular defects and atomic stepping characteristics of the nanostructure, this chain-like nanostructure has many of the best (111) facets and elemental segregations. As can be seen from the scanning transmission electron microscopy-EDS (STEM-EDS) elemental mapping of the Pt-Ni PNCs (Fig. 3 h–j), Pt is uniformly distributed and located at the surface, while Ni is relatively concentrated in the center. This is further uncovered by line scans crossing an individual polyhedron and wire in different directions (Fig. 3k, l). A large number of atomic steps and (111) facets, Pt-rich surfaces, ultrasmall dimensions, and the ordered arrangement of polyhedron-wire-polyhedron combine to increase the number of active sites and enhance mass and charge transfer in electrocatalysis. The electrochemical properties of as-prepared Pt-Ni PNC is significantly better than those of other samples such as conventional 0D Pt-Ni NPs, 1D Pt-Ni NWs and commercial Pt/C, as shown in Fig. 3m. Multiple advanced characterization techniques have shown that the excellent performance of mixed-dimensional Pt-Ni PNCs mainly depends on their unique nanostructure. The nanostructure can alleviate the problem of agglomeration

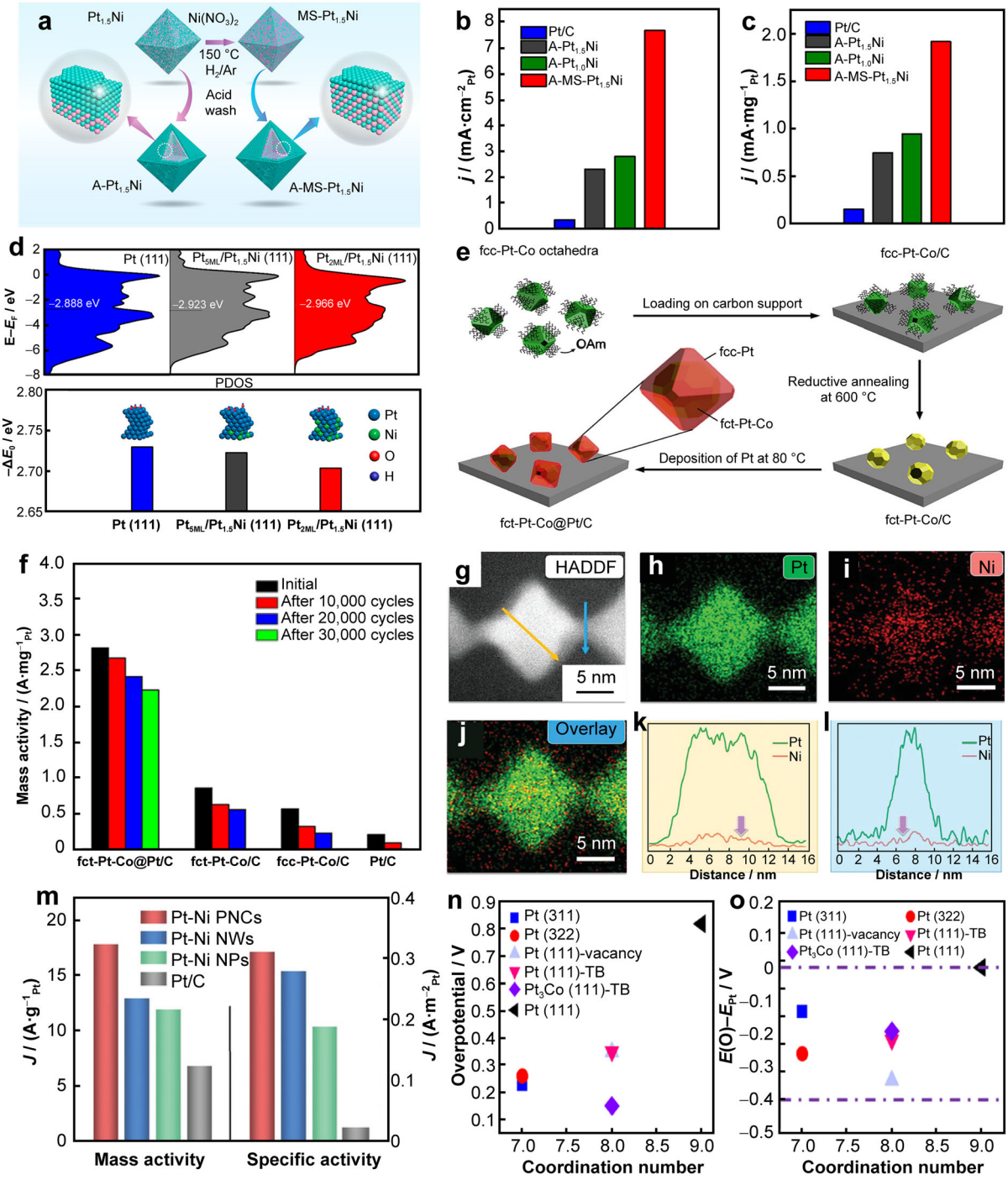

Fig. 3 **a** Schematic diagram of synthesis of octahedral PtNi alloy catalysts with Pt-rich shells; histogram of **b** MA and **c** SA of Pt/C, A-$Pt_{1.5}Ni$, A-$Pt_{1.0}Ni$, and A-MS-$Pt_{1.5}Ni$ at 0.9 V (calculated from catalysts performing CV in Ar-saturated 0.1 mol·L^{-1} $HClO_4$ and LSV in O_2-saturated 0.1 mol·L^{-1} $HClO_4$); **d** densities of electronic states and OH^* binding energy on (111) crystal plane of Pt/C, A-$Pt_{1.5}Ni$, and A-MS-$Pt_{1.5}Ni$ calculated by DFT. Reproduced with permission from Ref. [113]. Copyright 2020, American Chemical Society. **e** Schematic diagram of synthesis of fct-Pt-Co@Pt octahedral nanocrystal catalyst with an ultra-thin Pt layer; **f** MA of catalysts at 0.9 V vs. RHE before and after different cycles of ADT. Reproduced with permission from Ref. [114]. Copyright 2021, American Chemical Society. **g–j** HAADF-STEM images and corresponding EDS elemental mapping of Pt-Ni PNCs; **k**, **l** line-scanning analysis along yellow and blue arrows in **g**, where arrows represent Ni scarcity; **m** MA and SA of Pt-Ni PNCs, Pt-Ni NWCs, and Pt-Ni PNs at 0.9 V vs. RHE (calculated from catalysts performing CV in Ar-saturated 0.1 mol·L^{-1} $HClO_4$ and LSV in O_2-saturated 0.1 mol·L^{-1} $HClO_4$). Reproduced with permission from Ref. [118]. Copyright 2022, John Wiley and Sons. DFT-determined correlation of **n** overpotential and **o** atomic O binding energy relative to Pt (111) with coordination number of surface sites on each crystal plane during ORR. Reproduced with permission from Ref. [119]. Copyright 2022, American Chemical Society

Table 1 Summary of oxygen reduction performance indicators of some Pt-based catalysts

Electrocatalysts	Electrolyte	ECSA / ($m^2 \cdot g^{-1}$)	MA at 0.90 V (vs. RHE) / ($mA \cdot mg_{Pt}^{-1}$)	Refs.
Pt/3#	0.1 $mol \cdot L^{-1}$ $HClO_4$	92	150	[37]
Pt/EC300		55	86	
Pt/C 18		50	78	
Pt/C	0.1 $mol \cdot L^{-1}$ $HClO_4$	76.90	78.7	[39]
Pt/C-M (0.13, 180)		67.75	89.5	
Pt/CNT	0.1 $mol \cdot L^{-1}$ $HClO_4$	34.9	–	[58]
Pt/CNT-$Ti_3C_2T_x$ (1:1)		63.0	163	
Pt/CNT-$Ti_3C_2T_x$ (2:1)		34.2	50.4	
Pt/CNT-$Ti_3C_2T_x$ (1:2)		57.4	117	
Pt-CNT	0.1 $mol \cdot L^{-1}$ $HClO_4$	51.38	110	[59]
Pt-CNT@SnO_2-400		48.58	290	
Pt-Co/C	0.1 $mol \cdot L^{-1}$ $HClO_4$	49.2	640	[102]
Pt-Fe/C		50.9	470	
Pt-Ni/C		51.7	400	
2% Ga-Pt_3Co/C	0.1 $mol \cdot L^{-1}$ $HClO_4$	45.9	510	[104]
4% Ga-Pt_3Co/C		47.9	750	
8% Ga-Pt_3Co/C		54.3	670	
S-AuPbPt alloy NWNs	0.1 $mol \cdot L^{-1}$ $HClO_4$	140.35	590	[106]
PtFe/Pt-V NW	0.1 $mol \cdot L^{-1}$ KOH	25.6	3650	[109]
PtFe/Pt NW		5	–	
PtFe/Pt-V NW	0.1 $mol \cdot L^{-1}$ $HClO_4$	124.5	1100	[109]
PtFe/Pt NW		86.8	340	
fct-Pt-Co@Pt/C	0.1 $mol \cdot L^{-1}$ $HClO_4$	30.8	2820	[114]
fct-Pt-Co/C		24.9	860	
fcc-Pt-Co/C		23.4	570	
Pt-rich PtCo nanoflowers	0.1 $mol \cdot L^{-1}$ $HClO_4$	23.43	2630	[118]
PtCo nanoflowers		51.57	590	
PtCo NPs		45.42	190	
Pd-Pt nanoframes	0.1 $mol \cdot L^{-1}$ $HClO_4$	53.4	660	[123]
Pd-Pt tesseracts		44.9	1840	
Pd-Pt octapods		35.5	1320	
Pt-Co ND-NF	0.1 $mol \cdot L^{-1}$ $HClO_4$	35.6	939	[125]
Pt-Cu-Mn UNFs	0.1 $mol \cdot L^{-1}$ KOH	43.0	1450	[126]
Pt-Cu-Mn PNFs		36.6	850	
Al-Cu-Ni-Pt-Mn np-HEAs	0.1 $mol \cdot L^{-1}$ $HClO_4$	108.5	3466	[129]
$L1_0$-FePt	0.1 $mol \cdot L^{-1}$ KOH	–	1960	[138]
Pt_1Co_1-IMC@Pt/C	0.1 $mol \cdot L^{-1}$ $HClO_4$	43.5	530	[146]
Pt_1@Pt/NBP	0.1 $mol \cdot L^{-1}$ $HClO_4$	34.5	214	[156]
Pt_3Co@Pt-SACs	0.1 $mol \cdot L^{-1}$ $HClO_4$	40.4	1400	[157]
Pt_3Co/C		38.1	530	
Pt@Pt-SACs		53.6	330	

and dissolution of 0D small-sized Pt-Ni alloy nanocrystals, and enrich the surface atom steps and active surfaces of the 1D chain nanostructure. Wei et al. [119] prepared highly open Pt-rich PtCo nanoflowers catalysts assembled from ultrathin nanosheets by solvothermal and acid etching methods. The abundance of high-index facets and defects and the low-coordination site in the structure give it 17.5 and 38.7 times higher MA and SA than those of commercial Pt/C. DFT simulations were carried out to establish the relationship between ORR performance and different coordination numbers, d-band centers, overpotentials, and oxygen-binding energies. The simulation results are shown

in Fig. 3n, o, and it can be seen that the ORR performance of the low-coordination sites is much higher than that of the high coordination sites.

3.3 Hollow nanostructures

It is well known that for catalysts, only atoms on the surface or subsurface can participate in the reaction as active centers, while a large number of atoms located in the interior cannot participate as active centers [120]. To further reduce the amount of Pt used, the polyhedra were further processed and prepared as hollow nanostructures such as nanoframes (NFs), nanocages, and hollow nanodendrites (NDs) [121]. These hollow structures have a large specific surface area, highly exposed reaction sites, and short charge transfer distances, which can accelerate the slow ORR kinetics and further enhance the catalyst activity [122]. This section mainly describes the preparation and modification methods of Pt-based hollow nanostructures, including embedding NDs into NFs, using deformed hollow structures to enhance compressive strain, preparing Pt-based alloys into porous nanostructures, etc.

Preparing the catalyst into hollow nanostructures not only further reduces the amount of Pt used but also exposes more reaction sites, shortens the charge transfer distance, and improves the activity of the catalysts. Chen et al. [123] prepared a Pd-Pt hollow frame structure composed of double-shell cubes linked by body diagonally and obtained 11.6 times higher MA and 8.4 times higher SA than those of commercial samples. The study found that the Pt atoms migrated and rearranged during the etching process to reduce the surface energy, thereby improving the stability of the catalyst. Zhang et al. [124] transformed PtCu octahedral stars (PtCu OSs) into PtCu nested skeletal cubes (PtCu NSCs) by adding $Ni(acac)_2$ during the preparation process. The nanocrystals were then treated with acetic acid to remove surface material, including organic matter and oxides, and STEM images of the acid-treated PtCu NSCs (PtCu A-NSCs) are shown in Fig. 4a. As can be seen from the figure, PtCuA NSCs are composed of smaller skeletal cubes fully nested within larger skeletal cubes, with a spike protruding outward at each vertex of the outer skeletal cube. STEM-EDS elemental mapping of PtCu A-NSCs (Fig. 4b–e) shows a mostly uniform distribution of Pt (green), Cu (yellow), and Ni (red) throughout the nanocrystals. EDS line scans of the spike and ridge regions (highlighted in red in Panel a) reveal efficient Pt-rich structures on the ridge surface. Combined with XPS analysis, the Pt-rich structure will shift the center of the Pt d-band center downward, weakening the adsorption of oxygenated intermediates on the Pt sites. Among PtCu NSCs/C, Pt/C and PtCu A-NSCs/C, PtCu A-NSCs/C has the best binding energy to oxygen-containing intermediates and thus shows the highest ORR mass activity. EDS and XPS results showed that there were very few Ni^{2+} species in the NSCs, suggesting that the enhanced activity was independent of the use of Ni precursors during synthesis. So, the enhanced activity is due to the presence of the nested skeletal structure. The hollow cavities in NSCs allow for substantial mass transfer in ORR catalysis. PtCu A-NSC/C shows an excellent ORR stability after 5000/10000 cycles compared to the other three alloyed catalysts, as shown in Fig. 4f. This higher stability is due to the synergistic effect of the nanoalloy shape and the acid treatment process. The surface protrusions and peaks formed in the nanocrystals can counteract structural collapse and agglomeration of the catalyst, resulting in remarkably high activity and stability. Zhu et al. [125] synthesized PtCo-ND-NF catalysts consisting of internal NDs and an external NF by a simple one-pot method, and the schematic synthesis is shown in Fig. 4j. This highly open structure can effectively expose the active sites, promoting reaction kinetics and electron transport, which plays an important role in improving the activity of the catalyst. The outermost Pt skin protects the inner Pt-Co NDs and prevents the aggregation, dissolution of the catalysts, and separation from the support. Figure 4i shows the results of its electrochemical characterization. It can be seen that it has a mass activity about 5 times higher than that of the commercial sample and shows high stability in ADTs of 50,000 cycles.

The electronic structure of Pt can also be tuned by preparing the surface with compressive strain to reduce the d-band center and enhance the intrinsic activity of the catalysts. For example, Qin et al. [126] prepared ternary Pt-Cu-Mn nanoframes (Pt-Cu-Mn UNFs) with twins by the wet chemical method. They accurately measured the interplanar spacing of (111) planes in Pt-Cu-Mn UNFs and pentagram-shaped ternary Pt-Cu-Mn alloy (Pt-Cu-Mn PNFs) ridges using aberration-corrected STEM. Then, their lattice spacing was calculated using the intensity profile, and the calculation results are shown in Fig. 4g. It can be seen that the Pt-Cu-Mn UNFs have a compressive strain of approximately 1.5% compared to the Pt-Cu-Mn PNFs. Rotating disk electrode (RDE) tests in 0.1 $mol \cdot L^{-1}$ KOH showed that Pt-Cu-Mn UNFs had higher mass and specific activity than those of Pt-Cu-Mn PNFs and Pt/C, as shown in Fig. 4h. DFT calculations were performed to elucidate the increased ORR activity after compression. DFT calculations show that compression on the surface of Pt-Cu-Mn UNFs can weaken the binding and adsorption strengths of oxygen-containing intermediates, which play an important role in enhancing their ORR activity. Gong et al. [127] also prepared hollow-structured PtFe alloy catalysts with compressively strained Pt surfaces. When the Pt loading is only 0.86%, the MA and SA of the catalyst can

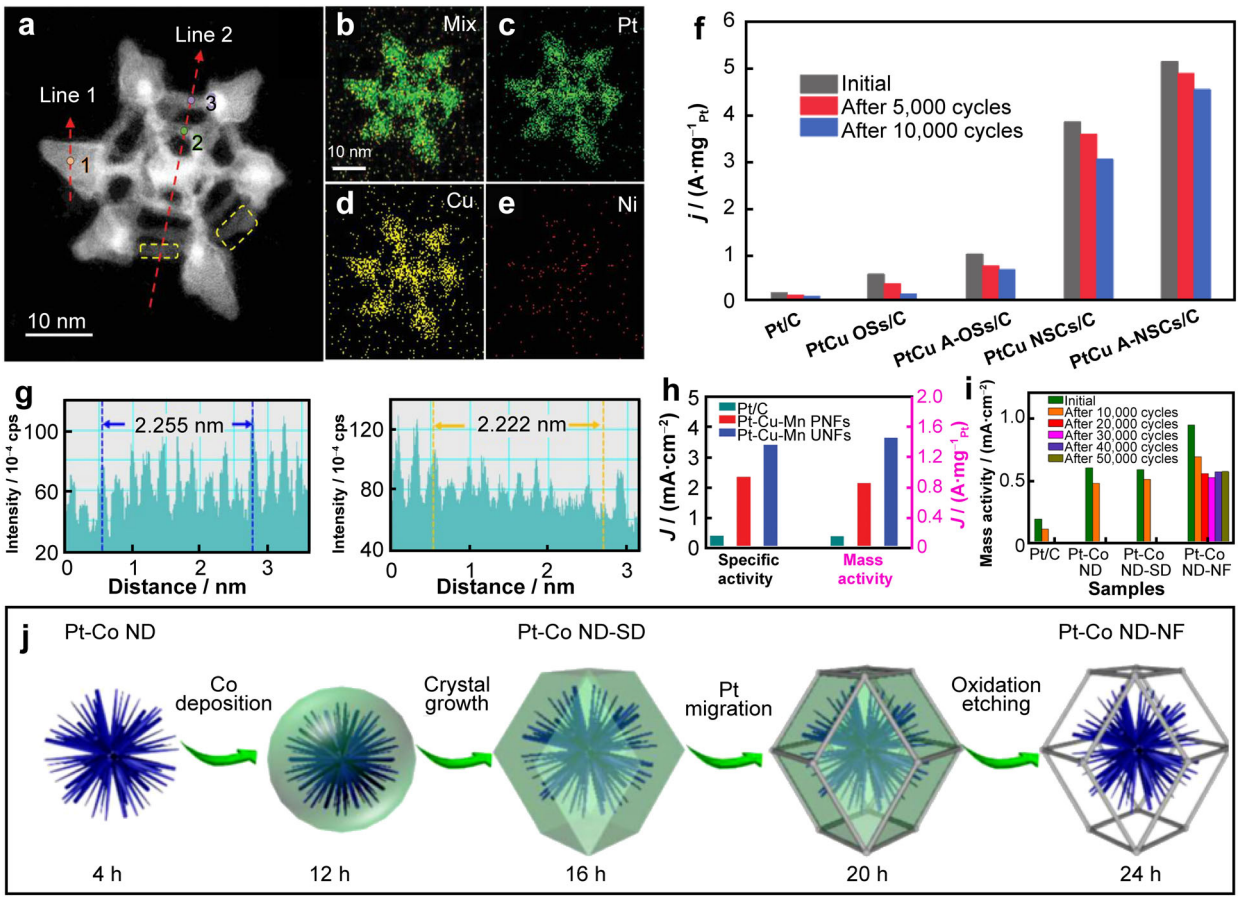

Fig. 4 **a** STEM image of PtCu A-NSCs; **b–e** corresponding EDS elemental mappings; **f** histogram of MA of PtCu A-NSCs and other catalysts at 0.9 V vs. RHE before and after ADTs in 0.1 mol·L^{-1} $HClO_4$ solution. Reproduced with permission from Ref. [124]. Copyright 2022, Advanced Science. **g** Lattice spacing calculation for Pt-Cu-Mn UNFs (left) and Pt-Cu-Mn PNFs (right); **h** MA and SA at 0.9 V vs. RHE obtained by RDE testing of Pt-Cu-Mn UNFs, Pt-Cu-Mn PNFs and commercial samples in 0.1 mol·L^{-1} KOH solution. Reproduced with permission from Ref. [126]. Copyright 2020, john Wiley and Sons. **i** MA of PtCo-ND-NF at 0.9 V vs. RHE before and after ADT in 0.1 mol·L^{-1} $HClO_4$ solution; **j** schematic diagram of synthesis of PtCo-ND-NF. Reproduced with permission from Ref. [125]. Copyright 2021, Elsevier

reach 2.3 and 2.7 times, respectively, that of the Pt/C commercial sample with 20% loading. This study is extremely important for reducing the amount of Pt and increasing the catalytic activity. Combining the unique high active specific surface area of the hollow structure with the intrinsic activity enhanced by the compressive strain, the catalyst exhibits excellent performance.

The use of de-alloying to give the alloy catalyst a nanoporous structure can also provide more active sites for ORR [128]. For example, Li et al. [129] used a top-down de-alloying synthesis method to obtain a series of nanoporous high-entropy alloys (np-HEAs) with Pt contents of about 20 at%–30 at% by controllably incorporating five incompatible metals into a nanoscale solid phase. Among them, Al-Cu-Ni-Pt-Mn np-HEAs exhibited the best ORR catalytic activity and electrochemical cycling durability, far exceeding that of commercial Pt/C catalysts. The Pt mass specific ECSA determined from the CO stripping curve is ~ 108.5 $m^2 \cdot g^{-1}$, which is much higher than that of commercial Pt/C (64.5 $m^2 \cdot g^{-1}$). It has a mass activity of 3466 $mA \cdot mg_{Pt}^{-1}$ obtained from electrochemical tests, which is much higher than that of the Pt/C catalyst. Yu et al. [130] prepared np-HEA containing 12 elements ($Mn_{70}Ni_{7.5}Cu_{7.5}Co_{4.2}V_{4.2}Fe_2Mo_2Pd_{0.5}Pt_{0.5}Au_{0.5}Ru_{0.5}Ir_{0.5}$), which we defined as np-HEA 12. Electrochemical test results showed that np-HEA 12 exhibited excellent ORR activity with a half-wave potential as high as 0.90 V, even higher than that of the commercial 20 wt% Pt/C (0.85 V). This shows that the many added elements have a synergistic effect on each other to enhance the performance of the catalyst, but the specific enhancement mechanism needs further research and exploration. The synergistic catalysis between porous Pt alloys encapsulated in defective graphitic carbon containing Co-N-C sites will optimize the reaction pathway of ORR and enhance the catalytic performance [131]. The preparation of the catalysts into hollow structures resulted

in a larger specific surface area, more reaction sites, and shorter charge transfer distances than polyhedral structures, which accelerated the slow ORR kinetics and not only reduced the amount of Pt used but also further enhanced the catalyst activity. In addition, the stability of the catalysts is improved during the preparation process as Pt atoms migrate and rearrange to reduce the surface energy.

4 Pt-based intergeneric compounds

In recent years, Pt-based intermetallic compounds have become a new class of ORR catalysts due to their higher activity and durability than that of Pt-based alloys [132, 133]. The ordered atomic arrangement in the intermetallic structure gives Pt-based intermetallic compounds stronger strain and ligand effects, and the long-range periodic crystal structure and well-defined stoichiometries of the intermetallic phases impart good chemical stability, giving them superior catalytic activity compared to alloys with disordered atomic arrangements [134–137]. However, intermetallic compounds are more difficult to produce as the transition from random alloy to intermetallic structure usually requires high-temperature annealing above 500 °C. High temperatures can accelerate metal sintering, leading to deformation and agglomeration of the nanostructure and the formation of larger particles [134]. This chapter reviews the research progress on intermetallic compounds, mainly focusing on solving the problems of atom migration, aggregation, grain growth, etc. during annealing. After that, we also summarized some methods to enhance the activity and durability of Pt-based intermetallic compound catalysts, such as encapsulation in carbon layers, combination with nanostructures.

Much researches have been done to solve the problems of atom migration and the agglomeration of intermetallic compounds during annealing. Yoo et al. [138] used the bimetallic compound M (M = Fe, Co, or Ni; bpy = 2,2′-bipyridine) on rGO, which thermally decomposed to form uniformly sized intermetallic compound $L1_0$-MPt grains with good stability. And Ma et al. [139] used a strong electrostatic adsorption method to make Pt and Co metal ion precursors strongly attached to the carbon support and controlled the size of the alloy PtCo nanocrystals by adjusting the pH value of the carbon support and precursor suspension. The strong adhesion of metal ion precursors ensured the anchoring of the PtCo NPs on carbon supports and inhibited atomic migration and sintering during their conversion to intermetallic phases, resulting in the preparation of PtCo intermetallic compounds with an average size of less than 3 nm. Luo et al. [140] prepared highly loaded ($\sim$ 50 wt%) Pt-Cu_3 intermetallic compound catalysts uniformly dispersed on rGO using NH_4OH as a traceless protectant with the assistance of the spray freeze-drying method as shown in Fig. 5a. The addition of NH_4OH was used to resist GO folding and easily removed during subsequent drying and annealing, while spray freeze drying ensured excellent dispersion of Pt and Cu precursors on GO. Figure 5b shows its TEM image and the inset shows the corresponding histogram of the diameter distribution. From the figure, it can be seen that the prepared catalyst has a uniform dispersion and a narrow particle size range, indicating that the added NH_4OH plays an effective role in preventing GO aggregation. Figure 5c shows the Gibbs free energy diagrams of the ORR process for both Pt(111) and $PtCu_3$(111) structures, where Pt and $PtCu_3$ have consistent downhill energy paths at $U = 0$ V (vs. RHE), indicating a spontaneous exothermic process. When $U = 1.23$ V_{RHE}, $PtCu_3$ has a lower energy barrier for the RDS, contributing to a significant improvement in ORR kinetics.

Preventing particle growth during the disordered-to-ordered transition of alloys is essential for the preparation of high-performance intermetallic compound catalysts. Some studies have found that intermetallic compounds can be encapsulated in the carbon layer. The outer carbon shell can not only prevent the growth of NPs during the sintering process but also protect the catalyst from poisoning during the electrochemical cycle, which can increase catalyst stability. Doping the carbon supports with other elements can further enhance the anchoring effect of carbon supports and inhibit the growth of particles. Hu et al. [141] encapsulated Pt-Fe ordered intermetallic nanoparticles (i-NPs) into a shell of N-doped carbon, which not only prevents agglomeration, exfoliation, or Ostwald ripening of the grains during electrochemical testing and high-temperature synthesis but also can be used to anchor the catalyst and improve its dispersion due to the strong coupling between the catalyst and the N-doped carbon shell. Electrochemical tests have shown that the catalyst has excellent durability, activity, and excellent anti-poisoning performance. Hu et al. [142] studied $PtCo_3$ intermetallic compounds encapsulated in hollow porous N-doped carbon spheres. They found that the outer carbon shell could not only inhibit the oxidation and growth of Co during high-temperature synthesis but also prevent Ostwald ripening and agglomeration of the catalyst during electrochemical processes. It is further demonstrated that the use of N-doped carbon for encapsulating intermetallic compounds can not only solve their grain growth problem during annealing, but the encapsulated carbon layer can also significantly enhance the durability of the catalyst during the ORR reaction. It has been found that when porous sulfur-doped carbon is supported with Pt intermetallic compounds, S and Pt form strong interactions that inhibit high-temperature sintering. Yang et al. [143] prepared a variety of Pt-based

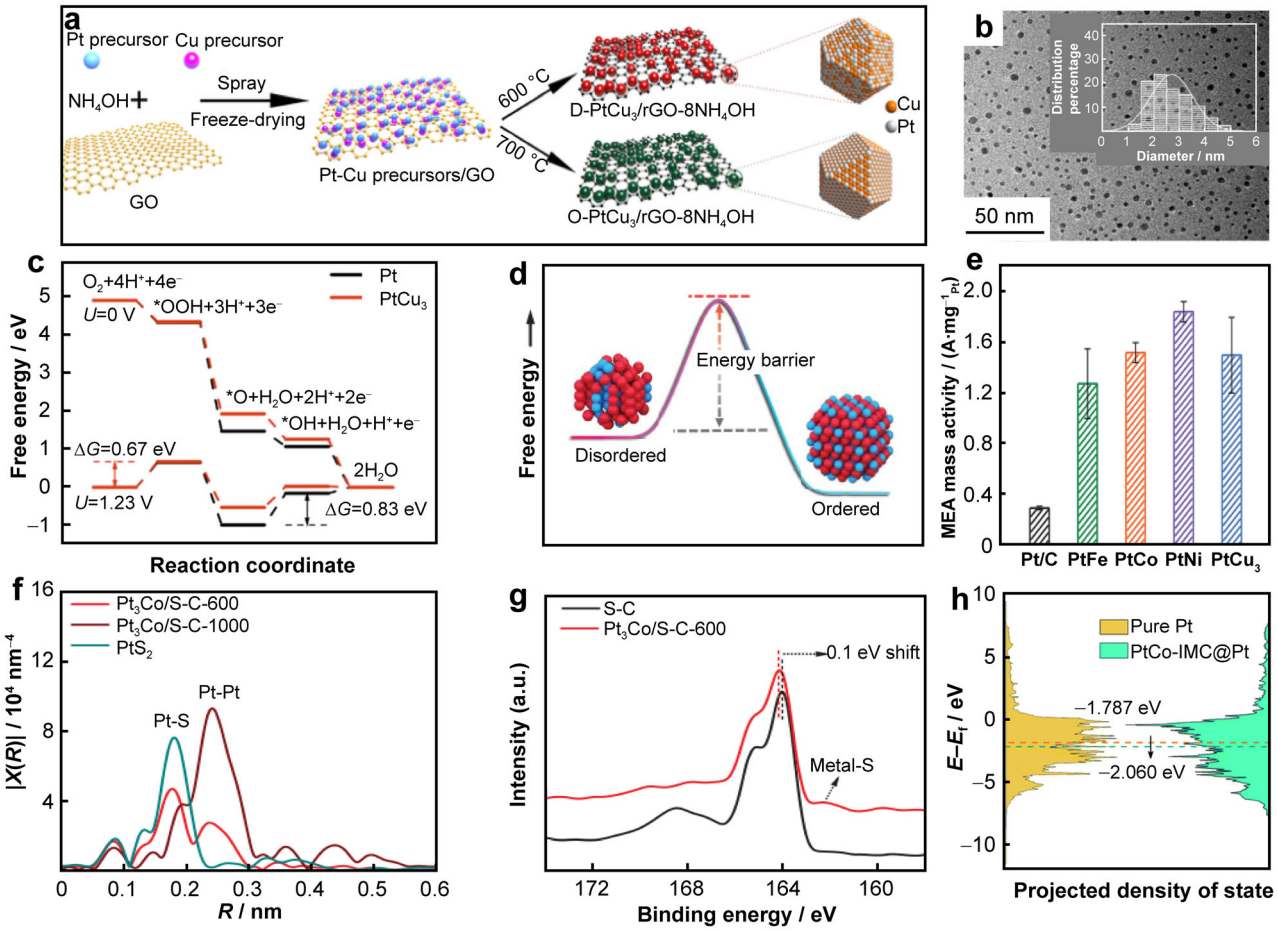

Fig. 5 **a** Schematic diagram of preparation of $PtCu_3$/rGO; **b** TEM image of O-$PtCu_3$/rGO-8NH_4OH and (inset) corresponding diameter distribution histogram; **c** DFT calculation results of Gibbs free energy diagram for ORR process of Pt (black line) and $PtCu_3$ (red line) at U = 0 and 1.23 V. Reproduced with permission from Ref. [140]. Copyright 2022, Elsevier. **d** Schematic diagram of kinetic energy barrier for transition from atomic disorder to atomic order; **e** cathodic MA of membrane electrode assemblies (MEAs) made with cathode catalysts of Pt/C and i-NP catalysts; **f** Fourier-transformed EXAFS data at Pt L_3-edge of Pt_3Co/S-C-600, Pt_3Co/S-C-1000, and PtS_2; **g** XPS spectra of Pt_3Co/S-C-600 and S-C, indicating electronic interaction between metals and S-C, where a.u. is arbitrary units. Reproduced with permission from Ref. [143]. Copyright 2021, the American Association for the Advancement of Science. **h** PDOS of Pt and Pt_1Co_1-IMC@Pt. Reproduced with permission from Ref. [146]. Copyright 2022, Royal Society of Chemistry

intermetallic compound nanoparticles (i-NPs) on porous S-doped carbon (S-C) supports. H_2PtCl_6 is first reduced by H_2 at low temperature (< 400 °C) to form Pt clusters and is anchored in S-C by doped sulfur through Pt-S bonds. Then, at high temperature (600 to 800 °C), Co was reduced and alloyed with Pt to form disordered Pt-Co NPs. To achieve the disordered-to-ordered transition, the kinetic barrier to atomic order must be overcome (Fig. 5d), so a high-temperature annealing process is necessary. After a high-temperature annealing treatment at 1000 °C, the disordered alloy is transformed into an atomically ordered Pt_3Co intermetallic structure driven by thermodynamics. As the temperature rises during the annealing process, the doped sulfur atoms gradually leave the carbon matrix, causing a slight sintering. While the average size of Pt_3Co i-NPs is still less than 5 nm, this may be due to the chemical limiting effect of the residual sulfur sites enriched around the alloy grains on the S-C support. And in the subsequent electrochemical tests, the MA of the prepared PtFe, PtCo, PtNi and $PtCu_3$ i-NPs were all much higher than those of the commercial Pt/C (Fig. 5e). To investigate the chemical interactions between S and Pt therein, the Fourier transform extended X-ray absorption fine structure (EXAFS) characterization (Fig. 5f) revealed that Pt-S bonds do exist in Pt_3Co/S-C. The XPS spectrum of Pt_3Co/S-C-600 and S-C (Fig. 5g) show that the S 2p peak shifts by 0.1 eV toward a higher binding energy than that with the pristine S-C support. This indicates electron transfer from sulfur to metal, indicating electronic interaction between metal and S-C. These characterizations confirm the existence of Pt-S bonds in Pt_3Co/S-C, which can increase the adhesion energy of i-NPs on S-C supports and also retard Ostwald

ripening, particle migration, and coalescence. This suppresses interparticle sintering.

Some researchers dispersed the metal elements into the carbon support at the atomic level and applied heat treatment after supporting Pt so that the metal elements diffused into the Pt lattice to form small-sized Pt intermetallic compounds. For example, Guo et al. [144] dispersed Co atoms into carbon supports to obtain Co-N-C supports. Pt was loaded on the support with polyol reduction, and then heat-treated to diffuse the Co atoms embedded in the Co-N-C support into the Pt lattice, thereby achieving formation of ultra-small PtCo i-NPs. The diffusive migration of Co atoms into the Pt nanolattice causes the Pt lattice to contract, and the compressive strain leads to a lower d-band center, which helps to weaken the adsorption strength of the oxygen-based intermediates on the Pt surface. The PtCo/Co-N-C catalysts prepared with the dual effects of enhanced EMSI and alloying effects have excellent performance, with a half-wave potential of 0.921 V and MA of 0.700 A $\cdot mg_{Pt}^{-1}$ @0.9 V.

Combining the advantages of intermetallic compounds and nanostructures, the preparation of intermetallic compounds into unique nanostructures can further enhance the activity and stability of catalysts. Kim et al. [134] prepared a PtCu NF with an atomically ordered intermetallic structure (O-PtCu NF/C). Electrochemical characterization showed that the MA and SA of the catalysts were 2.1 and 2.2 times that of the disordered PtCu NFs and 7.7 and 14.2 times that of the commercial sample, respectively. This study confirms the feasibility of combining intermetallic compounds and nanostructures and that the synergy between the two is effective in improving the activity and stability of the catalyst. Yang et al. [145] used silica to protect PtFeIr nanowires from deformation during the high-temperature phase transition and prepared the face-centered tetragonal-ordered PtFeIr intermetallic nanowire catalysts (fct-PtFeIr/C) with an average diameter of 2.6 nm. The MA of the prepared fct-PtFeIr/C was about twice that of the disordered face-centered cubic structure of PtFeIr nanowires and about 10 times that of commercial Pt/C. Moreover, the structure and electrochemical performance of fct-PtFeIr/C remained unchanged after the stability test, showing the advantage of the ordered structure. The Pt-rich layer structure also had a good effect on strengthening intermetallic compounds. Cheng et al. [146] used cobalt oxide-assisted structure evolution to successfully synthesize Pt_1Co_1 intermetallic compound and Pt-rich shell catalyst (Pt_1Co_1-IMC@Pt/C). And then, they used DFT calculations to investigate the enhancement mechanisms in terms of their ORR activity and durability. Figure 5h shows the projected density of states (PDOS) of pure Pt and Pt_1Co_1-IMC@Pt. It can be seen that Pt_1Co_1-IMC@Pt has a lower d-band center than pure Pt, indicating that the antibonding orbitals are more electron filled and have weaker oxygen adsorption. By simulating the energy distribution of pure Pt and Pt_1Co_1-IMC@Pt during the ORR process, it was found that the adsorption energy of each reaction intermediate of Pt_1Co_1-IMC@Pt was significantly weakened compared to that of the pure Pt structure. This indicates that the ligand effect between Pt and Co atoms, triggered by the electron transfer from Co to Pt, greatly influences the adsorption behavior of the intermediate on the Pt site. Experiments and theories clearly show that the ordered arrangement of Pt-Co atoms gives the Pt surface a lower d-energy band center, which enhances the antioxidant properties of the Pt/Co sites and confers excellent oxygen resistance to the Co atoms, thus hindering the dissolution of Co atoms from Pt_1Co_1 NPs and improving the ORR activity and durability.

Although there are more studies on intermetallic compounds at this stage, there are still many aspects that need further investigation. For example, the specific mechanism of performance enhancement of intermetallic compounds requires further research and confirmation. The type of crystal structure that Pt forms with other metals and the principle of formation of this crystal structure remain to be explored. How different crystal structures affect the performance of catalysts is still unclear.

5 Pt-based single-atom catalysts

SACs are a new type of catalyst in which the active metal is anchored on a support in the form of single-atom dispersion [147]. They have the advantages of uniform active center height, adjustable coordination environment, and high atom utilization efficiency [148, 149]. However, due to the high surface energy of the highly dispersed atoms, the as-prepared SACs tend to agglomerate, so their loading is always low [150]. This chapter reviews the preparation and modification of SACs for ORR in recent years. The content mainly focuses on improving the dispersion of SACs and modifying single-atom alloy catalysts to improve their intrinsic activity.

There are a lot of studies to prove that the doping of carbon-based materials with heteroelements can anchor Pt atoms and improve the dispersion and loading of Pt on the support [151–153]. For example, Song et al. [28] used atomic layer deposition to synthesize Pt SACs on MOF-derived N-doped carbon (MOF-NC). HAADF-STEM and XAFS studies have shown that isolated Pt single-atoms tend to bind to N-doped sites on the support, making them highly dispersed. DFT of the ORR process on Pt SACs revealed that their ORR occurs in multiple channels instead of a single pathway, which greatly reduces the free energy

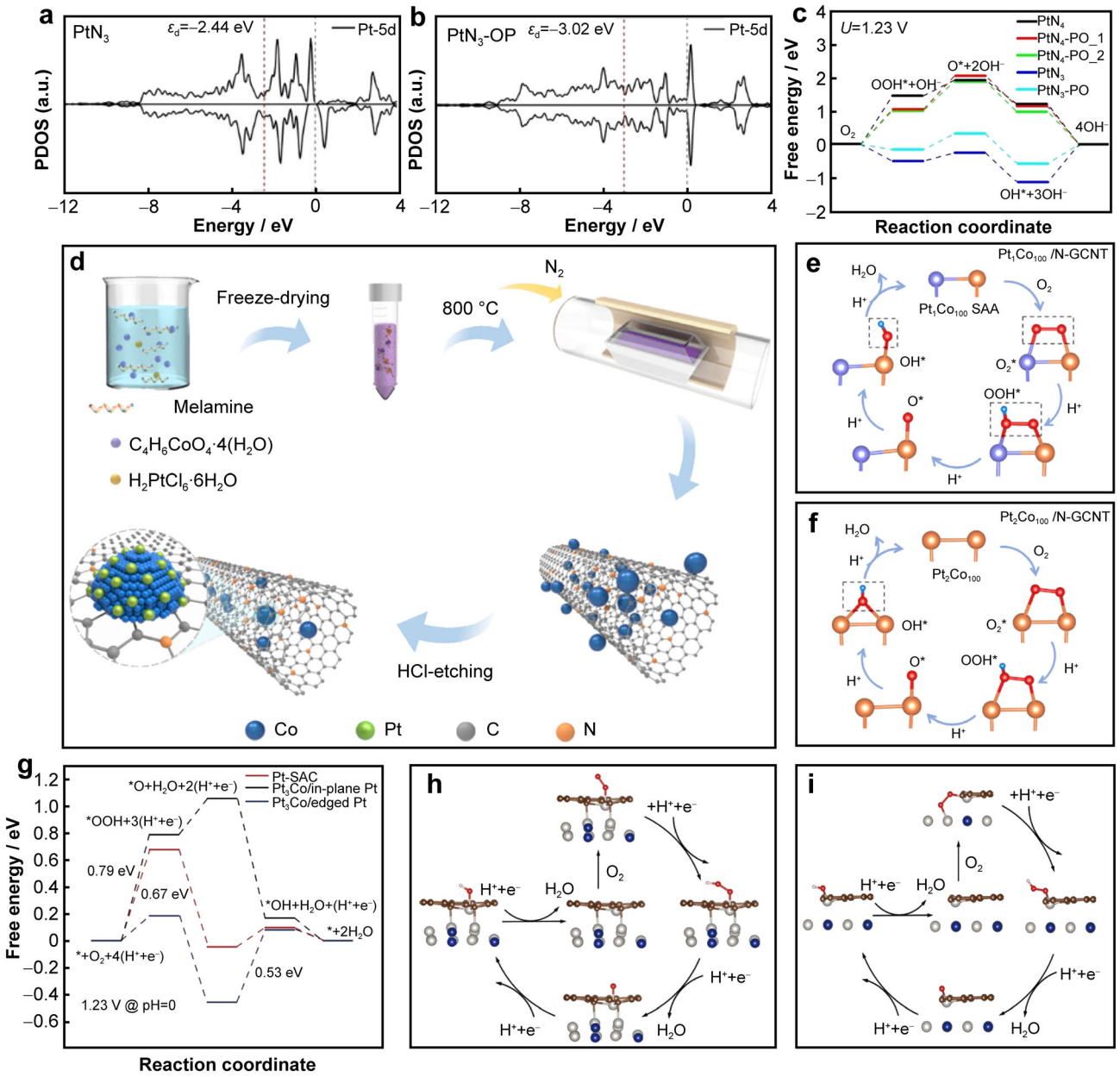

Fig. 6 PDOS of d orbitals of Pt atoms on **a** PtN_3 with 2OH and **b** PtN_3-PO with 2OH, where dotted gray line indicates Fermi level and d-band centers being denoted by dashed lines; **c** calculated free energy diagrams of ORR on PtN_x and PtN_x-PO catalysts at equilibrium potential (1.23 V) under alkaline conditions, where PtN_4-PO_1 and 2 indicate PO group located at two different α-C sites. Reproduced with permission from Ref. [154]. Copyright 2021, John Wiley and Sons. **d** Schematic illustration for synthetic process of Pt_1Co_n/N-GCNT encapsulated in a graphitic carbon nanotube; proposed ORR mechanism of **e** Pt_1Co_{100}/N-GCNT and **f** Pt_2Co_{100}/N-GCNT (gray, carbon; purple, cobalt; orange, platinum; red, oxygen; blue, hydrogen). Reproduced with permission from Ref. [155]. Copyright 2022, Elsevier. **g** Free energy diagram of different catalyst models; proposed ORR mechanisms based on **h** Pt_3Co/in-plane Pt model and **i** Pt_3Co/edged Pt model. Reproduced with permission from Ref. [157]. Copyright 2022, American Chemical Society

change in the RDS and enhances the activity of Pt SACs toward ORR. Yang et al. [149] used a one-pot hydrothermal method to prepare C_4N to support Pt SACs. The study found that Pt formed Pt-N-C complexes with C_4N, which could not only help to disperse Pt atoms but also improve the stability of the catalyst, showing excellent performance. Researchers also often use P-doped C to anchor Pt. Zhu et al. [154] used N and P co-doped carbon as supports to prepare Pt SACs and found that the P atoms doped in them would coordinate with abundant lone electrons, thereby reducing the d-band center of Pt. The PDOS analysis is shown in Fig. 6a, b. P in PtN_3-PO induces a leftward shift of the PDOS of the 5d orbital by modulating the 5d orbital of Pt, giving PtN_3-PO a lower d-band center. This weakens

the binding of oxygen intermediates to PtN_3-PO, lowers the RDS energy barrier, and enhances ORR activity. The results of the DFT simulation are shown in Fig. 6c. In an alkaline environment, PtN_3PO has the lowest energy barrier in determining the rate, giving it the best ORR activity. This shows that the introduced P element can adjust the electronic structure of Pt, reduce the d-band center of Pt, and then increase the intrinsic activity of the catalyst.

An efficient four-electron ORR pathway is an important way to enhance catalytic efficiency, which is particularly important for SACs. Cheng et al. [155] encapsulated Pt-Co single-atom alloy catalysts into N-doped graphitized carbon nanotubes (N-GCNTs) to obtain Pt_1Co_n/N-GCNTs. The schematic diagram of the synthesis process is shown in Fig. 6d. Theoretical calculations proved that the unique Pt-Co double sites in the as-prepared Pt_1Co_{100}/N-GCNTs were favorable for the adsorption and dissociation of oxygen, especially for the adsorption of OOH^* intermediates and the dissociation of OH^* intermediates, thus forming an efficient four-electron ORR pathway, as shown in Fig. 6e, f. Liu et al. [156] reconstructed the coordination environment of these isolated Pt atoms by high-temperature pyrolysis of Pt_1/NBP supported on nitrogen-doped activated carbon, forming a unique nitrogen-anchored Pt single-atom active site (Pt_1@Pt/NBP). They also obtained an efficient four-electron ORR pathway, giving the catalyst fast ORR kinetics, good ORR performance, and stability. Liu et al. [157] utilized the synergistic effect of single-atoms and alloys to achieve an efficient and durable four-electron ORR pathway, and its free energy diagram is shown in Fig. 6g. The Pt_3Co NPs at the interface optimize the electronic structure of the edge single-atom Pt, which is more favorable for the adsorption of $^*OOH$ (and O_2 molecules), thus improving the performance. The detailed schemes of the ORR mechanism of in-plane and edge single-atom Pt are shown in Fig. 6h, i. Combining in situ Raman analysis and theoretical calculations, it is found that Pt_3Co core nanocrystals modulate the electron structures of the adjacent Pt single-atoms to facilitate the intermediate absorption for fast kinetics, allowing the catalyst to exhibit MA and SA 1 order of magnitude higher than that of commercial Pt/C. The Pt-SACs coating significantly reduced the dissolution of the Pt_3Co core, resulting in a half-wave potential drop of only 10 mV after 50,000 cycles, showing good durability.

In addition to carbon materials, MXenes are used as substrate materials for SACs because of their unique two-dimensional structure, high surface area, and high electronic conductivity. Kan et al. [158] investigated the ORR activity of recombinant SACs by recombining Pt single atom on 26 representative MXenes using first-principles calculations. They studied the stability of Pt atoms on the surface of MXenes by using the formation and diffusion energy barriers. The charge transfer analysis revealed that the Pt atom was not only the catalytic center of SACs but also the charge-transfer mediator between the MXenes substrate and the reactants. When using O-terminated MXenes as a support for loading, it usually ends in failure, but they are more stable than F-terminated MXenes and more suitable as supports. Kan et al. [159] investigated the reason for this by using first-principles calculations to analyze the influence of these two materials on catalyst performance when used as supports. The reason for this is that the charge density around Pt and C in O-terminated MXenes-supported catalysts is low, which seriously reduces the catalytic activity of Pt. In order to use O-terminated MXenes as supports to improve the stability of Pt SACs, they successfully constructed ordered bimetallic MXenes by leaving the Nb (or Cr) submetal in the outer layer and inserting a second submetal, M^*, with lower electronegativity than Nb (or Cr) in the middle layer. Owing to the lower electronegativity of the second submetal, Pt, C and O/F atoms gain more electrons from the bimetallic MXenes. $^*O$ species can gain more electrons from the bimetallic system and be further activated during the reaction, which significantly improves the catalytic efficiency.

6 Conclusion and prospective

In this paper, the research progress of Pt-based catalysts for ORR in recent years is reviewed. We describe in detail the preparation and modification methods of Pt-based catalysts (including Pt/C, Pt-based alloys, Pt-based intermetallic compounds, and Pt-based SACs) and the principles of improving their activity, with an emphasis on three nanostructures of Pt-based alloy catalysts. The use of spatial confinement, heteroelement doping, and the preparation of composite materials as supports can improve the degree of dispersion of Pt and increase the corrosion resistance of the support, which is very beneficial for improving the activity and durability of Pt/C catalysts. Alloying other elements with Pt can produce ligand effects and coordination benefits, and improve the intrinsic activity of the catalyst. And preparing it into a special nanostructure can not only enhance the ligand and coordination effects but also expose more active sites. The hollow structure can also provide a larger specific surface area and a more stable structure, further improving catalyst performance. Transforming disordered alloys into atomically ordered intermetallic compounds can result in lower d-band centers and more stable structures. The combination of intermetallic compounds and polyhedrons can combine the advantages of both, and greatly improve the activity and durability of the catalyst. SACs have been a research

hotspot since their discovery. In addition to increasing their loading capacity and improving their dispersion in the preparation process to improve their performance, they can also be alloyed with other elements to create single-atom alloy catalysts. This further enhances their activity and durability.

Many Pt-based catalysts with excellent performance have been developed after years of research. To promote commercial use, ORR catalysts need to make more efforts on the path of low Pt, high efficiency, stability, economy, and environmental protection. We can start with the following directions:

(I) Optimizing the preparation process and reduce manufacturing costs. The process cost of high-performance ORR catalysts is still relatively high, or the operation is complicated, and it is difficult to achieve commercial promotion.

(II) Based on theoretical research, the performance of catalysts can be improved while reducing costs. Alloying Pt with various elements to form HEAs can further improve the performance and durability of Pt-based alloy catalysts. However, there are still few studies on Pt-based HEAs at this stage, especially the influence of composition and structure on their properties, which have not been determined and requires further theoretical and experimental research. The combination of intermetallic compounds and nanostructures can also significantly improve the activity of catalysts, but at this stage, the mechanism for improving the performance of the components and structures needs to be further studied and the preparation process further optimized.

(III) Development of noble metal-free catalysts with excellent performance. Although there have been some researches on noble metal-free ORR catalysts at this stage, their activity and stability are still not up to commercial standards, and there is still a long way to go to achieve or even surpass the performance of Pt-based catalysts.

(IV) Accelerate the design and development of ORR catalysts using advanced artificial intelligence technology. The traditional development method of catalysts is based on the trial-and-error method, which requires a lot of time and economic cost and is highly accidental. In recent years, with the development of big data and supercomputers, advanced artificial intelligence technologies, such as machine learning and deep learning, have been widely used in materials research and development. They have powerful learning, data analysis, and prediction capabilities that can significantly shorten the materials development cycle and reduce the cost of trial and error. The use of these advanced artificial intelligence technologies in the development of ORR catalysts will certainly have broad development prospects.

Acknowledgements This work was supported by CITIC Dameng Mining Industries Limited -Guangxi University Joint Research Institute of Manganese Resources Utilization and Advanced Materials Technology, Guangxi University-CITIC Dameng Mining Industries Limited Joint Base of Postgraduate Cultivation, and State Key Laboratory of Featured Metal Materials and Life-cycle Safety for Composite Structures, and the National Natural Science Foundation of China (Nos.11364003 and 52102470), Guangxi Innovation Driven Development Project Grant (Nos. AA17204100 and AA18118052) and the Natural Science Foundation of Guangxi Province (No. 2018GXNSFAA138186).

Declarations

Conflict of interests The authors declare that they have no conflict of interest.

References

[1] Li J, Zhang L, Doyle-Davis K, Li R, Sun X. Recent advances and strategies in the stabilization of single-atom catalysts for electrochemical applications. Carbon Energy. 2020;2(4):488. https://doi.org/10.1002/cey2.74.

[2] Xu X, Zhang Y, Miao X. Synthesis and electrocatalytic performance of 3D coral-like NiCo-P. Chin J Rare Met. 2022;46(11):1449. https://doi.org/10.13373/j.cnki.cjrm.XY22080001.

[3] Zhang Z, Lei Y, Huang W. Recent progress in carbon-based materials boosting electrochemical water splitting. Chin Chem Lett. 2022;33(8):3623. https://doi.org/10.1016/j.cclet.2021.11.041.

[4] Arunachalam S, Kirubasankar B, Pan D, Liu H, Yan C, Guo Z, Angaiah S. Research progress in rare earths and their composites based electrode materials for supercapacitors. Green Energy Environ. 2020;5(3):259. https://doi.org/10.1016/j.gee.2020.07.021.

[5] Wan H, Ma W, Zhou K, Cao Y, Liu X, Ma R. Advanced silicon nanostructures derived from natural silicate minerals for energy storage and conversion. Green Energy Environ. 2022;7(2):205. https://doi.org/10.1016/j.gee.2021.04.001.

[6] Pan Y, Deng FF, Fang Z, Chen HJ, Long Z, Hou XD. Integration of cryogenic trap to gas chromatography-sulfur chemiluminescent detection for online analysis of hydrogen gas for volatile sulfur compounds. Chin Chem Lett. 2021;32(11):3440. https://doi.org/10.1016/j.cclet.2021.05.067.

[7] Tian X, Lu XF, Xia BY, Lou XW. Advanced electrocatalysts for the oxygen reduction reaction in energy conversion technologies. Joule. 2020;4(1):45. https://doi.org/10.1016/j.joule.2019.12.014.

[8] Wang K, Li N, Yang Y, Ke S, Zhang Z, Dou M, Wang F. Effect of load-cycling amplitude on performance degradation for proton exchange membrane fuel cell. Chin Chem Lett. 2021;32(10):3159. https://doi.org/10.1016/j.cclet.2021.02.045.

[9] Wang Y, Ruiz Diaz DF, Chen KS, Wang Z, Adroher XC. Materials, technological status, and fundamentals of PEM fuel cells – a review. Mater Today. 2020;32:178. https://doi.org/10.1016/j.mattod.2019.06.005.

[10] Zhang J, Yuan Y, Gao L, Zeng G, Li M, Huang H. Stabilizing Pt-based electrocatalysts for oxygen reduction reaction: fundamental understanding and design strategies. Adv Mater. 2021;33(20):2006494. https://doi.org/10.1002/adma.202006494.
[11] Huang L, Zaman S, Tian X, Wang Z, Fang W, Xia BY. Advanced platinum-based oxygen reduction electrocatalysts for fuel cells. Acc Chem Res. 2021;54(2):311. https://doi.org/10.1021/acs.accounts.0c00488.
[12] Li CJ, Shan GC, Guo CX, Ma RG. Design strategies of Pd-based electrocatalysts for efficient oxygen reduction. Rare Met. 2023;42(6):1778. https://doi.org/10.1039/d0ta09092a.
[13] Dong M, Liu X, Jiang L, Zhu Z, Shu Y, Chen S, Dou Y, Liu P, Yin H, Zhao H. Cobalt-doped Mn_3O_4 nanocrystals embedded in graphene nanosheets as a high-performance bifunctional oxygen electrocatalyst for rechargeable Zn-air batteries. Green Energy Environ. 2020;5(4):499. https://doi.org/10.1016/j.gee.2020.06.022.
[14] Liu JB, Gong HS, Ye GL, Fei HL. Graphene oxide-derived single-atom catalysts for electrochemical energy conversion. Rare Met. 2022;41(5):1703. https://doi.org/10.1007/s12598-021-01904-z.
[15] Li S, Ho SH, Hua T, Zhou Q, Li F, Tang J. Sustainable biochar as an electrocatalysts for the oxygen reduction reaction in microbial fuel cells. Green Energy Environ. 2021;6(5):644. https://doi.org/10.1016/j.gee.2020.11.010.
[16] Chen L, Xu X, Yang W, Jia J. Recent advances in carbon-based electrocatalysts for oxygen reduction reaction. Chin Chem Lett. 2020;31(3):626. https://doi.org/10.1016/j.cclet.2019.08.008.
[17] Liu M, Xiao X, Li Q, Luo L, Ding M, Zhang B, Li Y, Zou J, Jiang B. Recent progress of electrocatalysts for oxygen reduction in fuel cells. J Colloid Interface Sci. 2022;607:791. https://doi.org/10.1016/j.jcis.2021.09.008.
[18] Shao M, Chang Q, Dodelet JP, Chenitz R. Recent advances in electrocatalysts for oxygen reduction reaction. Chem Rev. 2016;116(6):3594. https://doi.org/10.1021/acs.chemrev.5b00462.
[19] Shi Z, Yang W, Gu Y, Liao T, Sun Z. Metal-nitrogen-doped carbon materials as highly efficient catalysts: progress and rational design. Adv Sci. 2020;7(15):2001069. https://doi.org/10.1002/advs.202001069.
[20] Yang G, Choi W, Pu X, Yu C. Scalable synthesis of bi-functional high-performance carbon nanotube sponge catalysts and electrodes with optimum C–N–Fe coordination for oxygen reduction reaction. Energy Environ Sci. 2015;8(6):1799. https://doi.org/10.1039/c5ee00682a.
[21] Wang J, Kong H, Zhang J, Hao Y, Shao Z, Ciucci F. Carbon-based electrocatalysts for sustainable energy applications. Prog Mater Sci. 2021;116:100717. https://doi.org/10.1016/j.pmatsci.2020.100717.
[22] Quílez-Bermejo J, Morallón E, Cazorla-Amorós D. Metal-free heteroatom-doped carbon-based catalysts for ORR: a critical assessment about the role of heteroatoms. Carbon. 2020;165:434. https://doi.org/10.1016/j.carbon.2020.04.068.
[23] Ren X, Wang Y, Liu A, Zhang Z, Lv Q, Liu B. Current progress and performance improvement of Pt/C catalysts for fuel cells. J Mater Chem A. 2020;8(46):24284. https://doi.org/10.1039/d0ta08312g.
[24] Duan X, Cao F, Ding R, Li X, Li Q, Aisha R, Zhang S, Hua K, Rui Z, Wu Y, Li J, Li A, Liu J. Cobalt-doping stabilized active and durable sub-2 nm Pt Nanoclusters for low-Pt-loading PEMFC cathode. Adv Energy Mater. 2022;12(13):2103144. https://doi.org/10.1002/aenm.202103144.
[25] Jiménez-Morales I, Reyes-Carmona A, Dupont M, Cavaliere S, Rodlert M, Mornaghini F, Larsen MJ, Odgaard M, Zajac J, Jones DJ, Rozière J. Correlation between the surface characteristics of carbon supports and their electrochemical stability and performance in fuel cell cathodes. Carbon Energy. 2021;3(4):654. https://doi.org/10.1002/cey2.109.
[26] Zhao Z, Liu Z, Zhang A, Yan X, Xue W, Peng B, Xin HL, Pan X, Duan X, Huang Y. Graphene-nanopocket-encaged PtCo nanocatalysts for highly durable fuel cell operation under demanding ultralow-Pt-loading conditions. Nat Nanotechnol. 2022;17(9):968. https://doi.org/10.1038/s41565-022-01170-9.
[27] Xiong Y, Yang Y, DiSalvo FJ, Abruna HD. Synergistic Bimetallic metallic organic framework-derived Pt-Co oxygen reduction electrocatalysts. ACS Nano. 2020;14(10):13069. https://doi.org/10.1021/acsnano.0c04559.
[28] Song Z, Zhu YN, Liu H, Banis MN, Zhang L, Li J, Doyle--Davis K, Li R, Sham TK, Yang L, Young A, Botton GA, Liu LM, Sun X. Engineering the low coordinated Pt single atom to achieve the superior electrocatalytic performance toward oxygen reduction. Small. 2020;16(43):2003096. https://doi.org/10.1002/smll.202003096.
[29] Ren X, Lv Q, Liu L, Liu B, Wang Y, Liu A, Wu G. Current progress of Pt and Pt-based electrocatalysts used for fuel cells. Sustainable Energy Fuels. 2020;4(1):15. https://doi.org/10.1039/c9se00460b.
[30] Cheng Q, Hu C, Wang G, Zou Z, Yang H, Dai L. Carbon-defect-driven electroless deposition of Pt atomic clusters for highly efficient hydrogen evolution. J Am Chem Soc. 2020;142(12):5594. https://doi.org/10.1021/jacs.9b11524.
[31] Aftabuzzaman M, Shamsuddin Ahmed M, Matyjaszewski K, Kyu KH. Nanocrystal co-existed highly dense atomically disperse Pt@3D-hierarchical porous carbon electrocatalysts for tri-iodide and oxygen reduction reactions. Chem Eng J. 2022;446:137249. https://doi.org/10.1016/j.cej.2022.137249.
[32] Jauhar AM, Ma Z, Xiao M, Jiang G, Sy S, Li S, Yu A, Chen Z. Space-confined catalyst design toward ultrafine Pt nanoparticles with enhanced oxygen reduction activity and durability. J Power Sources. 2020;473:228607. https://doi.org/10.1016/j.jpowsour.2020.228607.
[33] Zhong H, Alberto Estudillo-Wong L, Gao Y, Feng Y, Alonso-Vante N. Oxygen vacancies engineering by coordinating oxygen-buffering CeO_2 with CoO nanorods as efficient bifunctional oxygen electrode electrocatalyst. J Energy Chem. 2021;59:615. https://doi.org/10.1016/j.jechem.2020.11.033.
[34] Trogadas P, Kapil N, Angel GMA, Kühl S, Strasser P, Brett DJL, Coppens MO. Rapid synthesis of supported single metal nanoparticles and effective removal of stabilizing ligands. J Mater Chem A. 2021;9(43):24283. https://doi.org/10.1039/d1ta06032e.
[35] Sun F, Su R, Zhou Y, Li H, Meng F, Luo Y, Zhang S, Zhang W, Zha B, Zhang S, Huo F. Synthesis of high-loading Pt/C electrocatalysts using a surfactant-assisted microwave discharge method for oxygen reduction reactions. ACS Appl Mater Interfaces. 2022;14(36):41079. https://doi.org/10.1021/acsami.2c11910.
[36] Ruiz-Camacho B, Palafox-Segoviano JA, Pérez-Díaz PJ, Medina-Ramírez A. Synthesis of supported Pt nanoparticles by sonication for ORR: effect of the graphene oxide-carbon composite. Int J Hydrogen Energy. 2021;46(51):26027. https://doi.org/10.1016/j.ijhydene.2021.03.143.
[37] Xie M, Chu T, Wang X, Li B, Yang D, Ming P, Zhang C. Effect of mesoporous carbon on oxygen reduction reaction activity as cathode catalyst support for proton exchange membrane fuel cell. Int J Hydrogen Energy. 2022;47(65):28074. https://doi.org/10.1016/j.ijhydene.2022.06.131.
[38] Labata MF, Li G, Ocon J, Chuang P-YA. Insights on platinum-carbon catalyst degradation mechanism for oxygen reduction reaction in acidic and alkaline media. J Power Sources. 2021;487:229356. https://doi.org/10.1016/j.jpowsour.2020.229356.

[39] Bai J, Ke S, Song J, Wang K, Sun C, Zhang J, Dou M. Surface engineering of carbon-supported platinum as a route to electrocatalysts with superior durability and activity for PEMFC cathodes. ACS Appl Mater Interfaces. 2022;14(4):5287. https://doi.org/10.1021/acsami.1c20823.
[40] Park KY, Sweers ME, Berner U, Hirth E, Downing JR, Hui J, Mailoa J, Johnston C, Kim S, Seitz LC, Hersam MC. Mitigating Pt loss in polymer electrolyte membrane fuel cell cathode catalysts using graphene nanoplatelet pickering emulsion processing. Adv Funct Mater. 2022;32(43):2205216. https://doi.org/10.1002/adfm.202205216.
[41] Zhang L, Lu P, Luo Y, Zheng JY, Ma W, Ding L-X, Wang H. Graphene-quantum-dot-composited platinum nanotube arrays as a dual efficient electrocatalyst for the oxygen reduction reaction and methanol electro-oxidation. J Mater Chem A. 2021;9(15):9609. https://doi.org/10.1039/d0ta12418d.
[42] Gan J, Zhang J, Zhang B, Chen W, Niu D, Qin Y, Duan X, Zhou X. Active sites engineering of Pt/CNT oxygen reduction catalysts by atomic layer deposition. J Energy Chem. 2020;45(C):59. https://doi.org/10.1016/j.jechem.2019.09.024.
[43] Meng QH, Hao C, Yan B, Yang B, Liu J, Shen PK, Tian ZQ. High-performance proton exchange membrane fuel cell with ultra-low loading Pt on vertically aligned carbon nanotubes as integrated catalyst layer. J Energy Chem. 2022;71:497. https://doi.org/10.1016/j.jechem.2022.03.018.
[44] Pajootan E, Omanovic S, Coulombe S. Controllable dry synthesis of binder-free nanostructured platinum electrocatalysts supported on multi-walled carbon nanotubes and their performance in the oxygen reduction reaction. Chem Eng J. 2021;426:131706. https://doi.org/10.1016/j.cej.2021.131706.
[45] Chen X, Niu K, Xue Z, Liu X, Liu B, Zhang B, Zeng H, Lv W, Zhang Y, Wu Y. Ultrafine platinum nanoparticles supported on N, S-codoped porous carbon nanofibers as efficient multifunctional materials for noticeable oxygen reduction reaction and water splitting performance. Nanoscale Adv. 2022;4(6):1639. https://doi.org/10.1039/d2na00014h.
[46] Sun Y, Li M, Qu X, Zheng S, Alvarez PJJ, Fu H. Efficient reduction of selenite to elemental selenium by liquid-phase catalytic hydrogenation using a highly stable multiwalled carbon nanotube-supported Pt catalyst coated by N-doped carbon. ACS Appl Mater Interfaces. 2021;13(25):29541. https://doi.org/10.1021/acsami.1c05101.
[47] Mardle P, Ji X, Wu J, Guan S, Dong H, Du S. Thin film electrodes from Pt nanorods supported on aligned N-CNTs for proton exchange membrane fuel cells. Appl Catal, B. 2020;260(C):118031. https://doi.org/10.1016/j.apcatb.2019.118031.
[48] Lu L, Deng H, Zhao Z, Xu B, Sun X. N-doped carbon nanotubes supported Pt nanowire catalysts for proton exchange membrane fuel cells. J Power Sources. 2022;529:231229. https://doi.org/10.1016/j.jpowsour.2022.231229.
[49] Dong Q, Mo Z, Wang H, Ji S, Wang X, Linkov V, Wang R. N-doped carbon networks containing inserted FeN_x@NC nanospheroids and bridged by carbon nanotubes as enhanced catalysts for the oxygen reduction reaction. ACS Sustainable Chem Eng. 2020;8(18):6979. https://doi.org/10.1021/acssuschemeng.0c00132.
[50] Liu X, Yang W, Chen L, Liu Z, Long L, Wang S, Liu C, Dong S, Jia J. Graphitic carbon nitride (g-C_3N_4)-derived bamboo-like carbon nanotubes/Co nanoparticles hybrids for highly efficient electrocatalytic oxygen reduction. ACS Appl Mater Interfaces. 2020;12(4):4463. https://doi.org/10.1021/acsami.9b18454.
[51] Tang F, Xia W, Zhang H, Zheng L, Zhao Y, Ge J, Tang J. Synthesis of Fe-doped carbon hybrid composed of CNT/flake-like carbon for catalyzing oxygen reduction. Nano Res. 2022;15(7):6670. https://doi.org/10.1007/s12274-022-4223-8.
[52] Wang Y, Liu Y, Yang H, Liu Y, Wu KH, Yang G. Ionic liquid derived Fe, N, B co-doped bamboo-like carbon nanotubes as an efficient oxygen reduction catalyst. J Colloid Interface Sci. 2020;579:637. https://doi.org/10.1016/j.jcis.2020.06.076.
[53] Choi JI, Kim HS, Sohn Y-J, Yim S-D, Alamgir FM, Jang SS. Density Functional theory study of oxygen reduction on graphene and platinum surfaces of Pt–graphene hybrids. ACS Appl Nano Mater. 2021;4(2):1067. https://doi.org/10.1021/acsanm.0c02625.
[54] Nechiyil D, Garapati MS, Shende RC, Joulie S, Neumeyer D, Bacsa R, Puech P, Ramaprabhu S, Bacsa W. Optimizing metal-support interphase for efficient fuel cell oxygen reduction reaction catalyst. J Colloid Interface Sci. 2020;561(C):439. https://doi.org/10.1016/j.jcis.2019.11.015.
[55] Chen LX, Jiang M, Lu Z, Gao C, Chen ZW, Singh CV. Two-dimensional graphdiyne-confined platinum catalyst for hydrogen evolution and oxygen reduction reactions. ACS Appl Mater Interfaces. 2021;13(40):47541. https://doi.org/10.1021/acsami.1c12054.
[56] Liu D, Zhang J, Liu D, Li T, Yan Y, Wei X, Yang Y, Yan S, Zou Z. N-doped graphene-coated commercial Pt/C catalysts toward high-stability and antipoisoning in oxygen reduction reaction. J Phys Chem Lett. 2022;13(8):2019. https://doi.org/10.1021/acs.jpclett.1c04005.
[57] Park C, Lee E, Lee G, Tak Y. Superior durability and stability of Pt electrocatalyst on N-doped graphene-TiO_2 hybrid material for oxygen reduction reaction and polymer electrolyte membrane fuel cells. Appl Catal, B. 2020;268:118414. https://doi.org/10.1016/j.apcatb.2019.118414.
[58] Xu C, Fan C, Zhang X, Chen H, Liu X, Fu Z, Wang R, Hong T, Cheng J. MXene ($Ti_3C_2T_x$) and carbon nanotube hybrid-supported platinum catalysts for the high-performance oxygen reduction reaction in PEMFC. ACS Appl Mater Interfaces. 2020;12(17):19539. https://doi.org/10.1021/acsami.0c02446.
[59] Li S, Liu J, Liang J, Lin Z, Liu X, Chen Y, Lu G, Wang C, Wei P, Han J, Huang Y, Wu G, Li Q. Tuning oxygen vacancy in SnO_2 inhibits Pt migration and agglomeration towards high-performing fuel cells. Appl Catal, B. 2023;320:122017. https://doi.org/10.1016/j.apcatb.2022.122017.
[60] Jung WS, Lee WH, Oh H-S, Popov BN. Highly stable and ordered intermetallic PtCo alloy catalyst supported on graphitized carbon containing Co@CN for oxygen reduction reaction. J Mater Chem A. 2020;8(38):19833. https://doi.org/10.1039/d0ta05182a.
[61] Kregar A, Tavčar G, Kravos A, Katrašnik T. Predictive system-level modeling framework for transient operation and cathode platinum degradation of high temperature proton exchange membrane fuel cells. ApEn. 2020;263:114547. https://doi.org/10.1016/j.apenergy.2020.114547.
[62] Sandbeck DJS, Inaba M, Quinson J, Bucher J, Zana A, Arenz M, Cherevko S. Particle size effect on platinum dissolution: practical considerations for fuel cells. ACS Appl Mater Interfaces. 2020;12(23):25718. https://doi.org/10.1021/acsami.0c02801.
[63] Sandbeck DJS, Secher NM, Speck FD, Sørensen JE, Kibsgaard J, Chorkendorff I, Cherevko S. Particle size effect on platinum dissolution: considerations for accelerated stability testing of fuel cell catalysts. ACS Catal. 2020;10(11):6281. https://doi.org/10.1021/acscatal.0c00779.
[64] Wang S, Xiong X, Zou X, Ding K, Pang Z, Xu Q, Zhou Z, Lu X. Unraveling the dissolution mechanism of platinum and silver electrodes during composite electrodeposition in a deep eutectic solvent. J Mater Chem A. 2020;8(8):4354. https://doi.org/10.1039/c9ta13577d.
[65] Bogar M, Yakovlev Y, Sandbeck DJS, Cherevko S, Matolínová I, Amenitsch H, Khalakhan I. Interplay among dealloying,

ostwald ripening, and coalescence in Pt_xNi_{100-x} bimetallic alloys under fuel-cell-related conditions. ACS Catal. 2021; 11(18):11360. https://doi.org/10.1021/acscatal.1c01111.
[66] Kovtunenko VA, Karpenko-Jereb L. Study of voltage cycling conditions on Pt oxidation and dissolution in polymer electrolyte fuel cells. J Power Sources. 2021;493: 229693. https://doi.org/10.1016/j.jpowsour.2021.229693.
[67] Goswami N, Grunewald JB, Fuller TF, Mukherjee PP. Mechanistic interactions in polymer electrolyte fuel cell catalyst layer degradation. J Mater Chem A. 2022;10(28):15101. https://doi.org/10.1039/d2ta02177c.
[68] Wu Y-F, Ma J-W, Huang Y-H. Enhancing oxygen reduction reaction of Pt–Co/C nanocatalysts via synergetic effect between Pt and Co prepared by one-pot synthesis. Rare Met. 2022;42(1):146. https://doi.org/10.1007/s12598-022-02119-6.
[69] Cheng W-Z, Liang J-L, Yin H-B, Wang Y-J, Yan W-F, Zhang J-N. Bifunctional iron-phtalocyanine metal–organic framework catalyst for ORR, OER and rechargeable zinc–air battery. Rare Met. 2020;39(7):815. https://doi.org/10.1007/s12598-020-01440-2.
[70] Shu C, Tan Q, Deng C, Du W, Gan Z, Liu Y, Fan C, Jin H, Tang W, Yang Xd, Yang X, Wu Y. Hierarchically mesoporous carbon spheres coated with a single atomic Fe-N-C layer for balancing activity and mass transfer in fuel cells. Carbon Energy. 2021;4(1):1. https://doi.org/10.1002/cey2.136.
[71] Lykhach Y, Skála T, Neitzel A, Tsud N, Beranová K, Prince KC, Matolín V, Libuda J. Nanoscale architecture of ceria-based model catalysts: Pt-Co nanostructures on well-ordered CeO_2(111) thin films. Chin J Catal. 2020;41(6):985. https://doi.org/10.1016/s1872-2067(19)63462-5.
[72] Chen J, Qian G, Chu B, Jiang Z, Tan K, Luo L, Li B, Yin S. Tuning d-band center of Pt by PtCo-PtSn heterostructure for enhanced oxygen reduction reaction performance. Small. 2022; 18(12):2106773. https://doi.org/10.1002/smll.202106773.
[73] Li X, He Y, Cheng S, Li B, Zeng Y, Xie Z, Meng Q, Ma L, Kisslinger K, Tong X, Hwang S, Yao S, Li C, Qiao Z, Shan C, Zhu Y, Xie J, Wang G, Wu G, Su D. Atomic structure evolution of Pt-Co binary catalysts: single metal sites versus intermetallic nanocrystals. Adv Mater. 2021;33(48):2106371. https://doi.org/10.1002/adma.202106371.
[74] Tetteh EB, Gyan-Barimah C, Lee HY, Kang TH, Kang S, Ringe S, Yu JS. Strained Pt(221) facet in a PtCo@Pt-rich catalyst boosts oxygen reduction and hydrogen evolution activity. ACS Appl Mater Interfaces. 2022;14(22):25246. https://doi.org/10.1021/acsami.2c00398.
[75] Chen Q, Chen Z, Ali A, Luo Y, Feng H, Luo Y, Tsiakaras P, Kang SP. Shell-thickness-dependent Pd@PtNi core–shell nanosheets for efficient oxygen reduction reaction. Chem Eng J. 2022;427:131565. https://doi.org/10.1016/j.cej.2021.131565.
[76] Lee WJ, Bera S, Woo HJ, Hong W, Park JY, Oh SJ, Kwon SH. Atomic layer deposition enabled PtNi alloy catalysts for accelerated fuel-cell oxygen reduction activity and stability. Chem Eng J. 2022;442(P1):136123. https://doi.org/10.1016/j.cej.2022.136123.
[77] Liao Y, Li J, Zhang S, Chen S. High index surface-exposed and composition-graded $PtCu_3$@Pt_3Cu@Pt nanodendrites for high-performance oxygen reduction. Chin J Catal. 2021;42(7): 1108. https://doi.org/10.1016/s1872-2067(20)63735-4.
[78] Luo M, Qin Y, Li M, Sun Y, Li C, Li Y, Yang Y, Lv F, Wu D, Zhou P, Guo S. Interface modulation of twinned PtFe nanoplates branched 3D architecture for oxygen reduction catalysis. Sci Bull (Beijing). 2020;65(2):97. https://doi.org/10.1016/j.scib.2019.10.012.
[79] Liu X, Hao S, Zheng G, Su Z, Wang Y, Wang Q, Lei L, He Y, Zhang X. Ultrasmall Pt_2Sr alloy nanoparticles as efficient bifunctional electrocatalysts for oxygen reduction and hydrogen evolution in acidic media. J Energy Chem. 2022; 64(01):315. https://doi.org/10.1016/j.jechem.2021.04.065.
[80] Campos-Roldán CA, Pailloux F, Blanchard P-Y, Jones DJ, Rozière J, Cavaliere S. Rational design of carbon-supported platinum-gadolinium nanoalloys for oxygen reduction reaction. ACS Catal. 2021;11(21):13519. https://doi.org/10.1021/acscatal.1c02449.
[81] Tetteh EB, Lee HY, Shin CH, Kim Sh, Ham HC, Tran TN, Jang JH, Yoo SJ, Yu JS. New PtMg alloy with durable electrocatalytic performance for oxygen reduction reaction in proton exchange membrane fuel cell. ACS Energy Lett. 2020; 5(5):1601. https://doi.org/10.1021/acsenergylett.0c00184.
[82] Zhang L, Wang Q, Li L, Banis MN, Li J, Adair K, Sun Y, Li R, Zhao ZJ, Gu M, Sun X. Single atom surface engineering: a new strategy to boost electrochemical activities of Pt catalysts. Nano Energy. 2022;93:106813. https://doi.org/10.1016/j.nanoen.2021.106813.
[83] Kluge RM, Haid RW, Riss A, Bao Y, Seufert K, Schmidt TO, Watzele SA, Barth JV, Allegretti F, Auwärter W, Calle-Vallejo F, Bandarenka AS. A trade-off between ligand and strain effects optimizes the oxygen reduction activity of Pt alloys. Energy Environ Sci. 2022;15(12):5181. https://doi.org/10.1039/d2ee01850k.
[84] Ze H, Chen X, Wang XT, Wang YH, Chen QQ, Lin JS, Zhang YJ, Zhang XG, Tian ZQ, Li JF. Molecular insight of the critical role of ni in pt-based nanocatalysts for improving the oxygen reduction reaction probed using an in situ sers borrowing strategy. J Am Chem Soc. 2021;143(3):1318. https://doi.org/10.1021/jacs.0c12755.
[85] Hu B, Yuan J, Zhang J, Shu Q, Guan D, Yang G, Zhou W, Shao Z. High activity and durability of a Pt-Cu-Co ternary alloy electrocatalyst and its large-scale preparation for practical proton exchange membrane fuel cells. Compos B. 2021;222: 109082. https://doi.org/10.1016/j.compositesb.2021.109082.
[86] Dukic T, Moriau LJ, Pavko L, Kostelec M, Prokop M, Ruiz--Zepeda F, Sala M, Drazic G, Gatalo M, Hodnik N. Understanding the crucial significance of the temperature and potential window on the stability of carbon supported Pt-alloy nanoparticles as oxygen reduction reaction electrocatalysts. ACS Catal. 2022;12(1):101. https://doi.org/10.1021/acscatal.1c04205.
[87] Shen J, Hu Z, Chen K, Chen C, Zhu Y, Li C. Platinum based high entropy alloy oxygen reduction electrocatalysts for proton exchange membrane fuel cells. Mater Today Nano. 2023;21: 100282. https://doi.org/10.1016/j.mtnano.2022.100282.
[88] Zhang W, Feng X, Mao ZX, Li J, Wei Z. Stably immobilizing Sub-3 nm high-entropy Pt alloy nanocrystals in porous carbon as durable oxygen reduction electrocatalyst. Adv Funct Mater. 2022;32(44):2204110. https://doi.org/10.1002/adfm.202204110.
[89] Zhao P, Zhang B, Hao X, Yi W, Chen J, Cao Q. Rational design and synthesis of adjustable Pt and Pt-based 3D-nanoframeworks. ACS Appl Energy Mater. 2022;5(1):942. https://doi.org/10.1021/acsaem.1c03337.
[90] Yu Y, Xia F, Wang C, Wu J, Fu X, Ma D, Lin B, Wang J, Yue Q, Kang Y. High-entropy alloy nanoparticles as a promising electrocatalyst to enhance activity and durability for oxygen reduction. Nano Res. 2022;15(9):7868. https://doi.org/10.1007/s12274-022-4432-1.
[91] Zhu J, Elnabawy AO, Lyu Z, Xie M, Murray EA, Chen Z, Jin W, Mavrikakis M, Xia Y. Facet-controlled Pt–Ir nanocrystals with substantially enhanced activity and durability towards oxygen reduction. Mater Today. 2020;35:69. https://doi.org/10.1016/j.mattod.2019.11.002.
[92] Gong S, Sun M, Lee Y, Becknell N, Zhang J, Wang Z, Zhang L, Niu Z. Bulk-like Pt(100)-oriented ultrathin surface:

combining the merits of single crystals and nanoparticles to boost oxygen reduction reaction. Angew Chem Int Ed Engl. 2023;62(4):202214516. https://doi.org/10.1002/anie.202214516.
[93] Lutian Z, Cehuang F, Liuxuan L, Jiabin Y, Lu A, Xiaohui Y, Shuiyun S, Junliang Z. Electrochemical synthesis of monodispersed and highly alloyed PtCo nanoparticles with a remarkable durability towards oxygen reduction reaction. Appl Catal, B. 2022;318:121831. https://doi.org/10.1016/j.apcatb.2022.121831.
[94] Xiao F, Wang Q, Xu GL, Qin X, Hwang I, Sun CJ, Liu M, Hua W, Wu Hw, Zhu S, Li JC, Wang JG, Zhu Y, Wu D, Wei Z, Gu M, Amine K, Shao M. Atomically dispersed Pt and Fe sites and Pt–Fe nanoparticles for durable proton exchange membrane fuel cells. Nat Catal. 2022;5(6):503. https://doi.org/10.1038/s41929-022-00796-1.
[95] Daimon H, Yamazaki SI, Asahi M, Ioroi T, Inaba M. A strategy for drastic improvement in the durability of Pt/C and PtCo/C alloy catalysts for the oxygen reduction reaction by melamine surface modification. ACS Catal. 2022;12(15):8976. https://doi.org/10.1021/acscatal.2c01942.
[96] Rao P, Luo J, Li J, Huang W, Sun W, Chen Q, Jia C, Liu Z, Deng P, Shen Y, Tian X. One-dimensional PtFe hollow nanochains for the efficient oxygen reduction reaction. Carbon Energy. 2022;4(6):1003. https://doi.org/10.1002/cey2.192.
[97] Yuan Y, Zhang Q, Li Y, Lv L, Hou Y, Li G, Fu J, Yang L, Bai Z. Beads-on-string hierarchical structured electrocatalysts for efficient oxygen reduction reaction. Carbon Energy. 2022;5(2):1. https://doi.org/10.1002/cey2.253.
[98] Xu H, Shang H, Wang C, Du Y. Ultrafine Pt-based nanowires for advanced catalysis. Adv Funct Mater. 2020;30(28):2000793. https://doi.org/10.1002/adfm.202000793.
[99] Niu H, Xia C, Huang L, Zaman S, Maiyalagan T, Guo W, You B, Xia BY. Rational design and synthesis of one-dimensional platinum-based nanostructures for oxygen-reduction electrocatalysis. Chin J Catal. 2022;43(6):1459. https://doi.org/10.1016/s1872-2067(21)63862-7.
[100] Wang Q, Tian H, Yu Y, Li J, Rao P, Li R, Du Y, Jia C, Luo J, Deng P, Shen Y, Tian X. Synthesis and design of a highly stable platinum nickel electrocatalyst for the oxygen reduction reaction. ACS Appl Mater Interfaces. 2021;13(44):52681. https://doi.org/10.1021/acsami.1c16375.
[101] Cheng N, Zhang L, Zhou Y, Yu S, Chen L, Jiang H, Li C. A general carbon monoxide-assisted strategy for synthesizing one-nanometer-thick Pt-based nanowires as effective electrocatalysts. J Colloid Interface Sci. 2020;572:170. https://doi.org/10.1016/j.jcis.2020.03.083.
[102] Lei W, Li M, He L, Meng X, Mu Z, Yu Y, Ross FM, Yang W. A general strategy for bimetallic Pt-based nano-branched structures as highly active and stable oxygen reduction and methanol oxidation bifunctional catalysts. Nano Res. 2020;13(3):638. https://doi.org/10.1007/s12274-020-2666-3.
[103] Cao H, Cao J, Wang F, Di S, Zhu H, Pu M, Bulanova A. Composition-tunable PtCu porous nanowires as highly active and durable catalyst for oxygen reduction reaction. Int J Hydrogen Energy. 2021;46(35):18284. https://doi.org/10.1016/j.ijhydene.2021.02.208.
[104] Li M, Zhao Z, Xia Z, Yang Y, Luo M, Huang Y, Sun Y, Chao Y, Yang W, Yang W, Yu Y, Lu G, Guo S. Lavender-like Ga-doped Pt_3Co nanowires for highly stable and active electrocatalysis. ACS Catal. 20 20;10(5):3018. https://doi.org/10.1021/acscatal.9b04419.
[105] Kong Z, Maswadeh Y, Vargas JA, Shan S, Wu ZP, Kareem H, Leff AC, Tran DT, Chang F, Yan S, Nam S, Zhao X, Lee JM, Luo J, Shastri S, Yu G, Petkov V, Zhong CJ. Origin of high activity and durability of twisty nanowire alloy catalysts under oxygen reduction and fuel cell operating conditions. JACS. 2020;142(3):1287. https://doi.org/10.1021/jacs.9b10239.
[106] Zhang X, Wang S, Wu C, Li H, Cao Y, Li S, Xia H. Synthesis of S-doped AuPbPt alloy nanowire-networks as superior catalysts towards the ORR and HER. J Mater Chem A. 2020;8(45):23906. https://doi.org/10.1039/d0ta06543a.
[107] Deng Z, Pang W, Gong M, Jin Z, Wang X. Revealing the role of mo doping in promoting oxygen reduction reaction performance of Pt_3Co nanowires. J Energy Chem. 2022;66(03):16. https://doi.org/10.1016/j.jechem.2021.06.018.
[108] Liu J, Liu S, Yan F, Wen Z, Chen W, Liu X, Liu Q, Shang J, Yu R, Su D, Shui J. Ultrathin nanotube structure for mass-efficient and durable oxygen reduction reaction catalysts in PEM fuel cells. J Am Chem Soc. 2022;144(41):19106. https://doi.org/10.1021/jacs.2c08361.
[109] Shi Y, Yang W, Gong W, Wang X, Zhou Y, Shen X, Wu Y, Di J, Zhang D, Li Q. Interconnected surface-vacancy-rich PtFe nanowires for efficient oxygen reduction. J Mater Chem A. 2021;9(21):12845. https://doi.org/10.1039/d1ta00972a.
[110] Kabiraz MK, Ruqia B, Kim J, Kim H, Kim HJ, Hong Y, Kim MJ, Kim YK, Kim C, Lee WJ, Lee W, Hwang GH, Ri HC, Baik H, Oh HS, Lee YW, Gao L, Huang H, Paek SM, Jo YJ, Choi CH, Han SW, Choi SI. Understanding the grain boundary behavior of bimetallic platinum-cobalt alloy nanowires toward oxygen electro-reduction. ACS Catal. 2022;12(6):3516. https://doi.org/10.1021/acscatal.1c05766.
[111] Lin R, Sun Y, Cai X, Zheng T, Liu X, Wang H, Liu S, Hao Z. Embedding Pt-Ni octahedral nanoparticles in the 3D nitrogen-doped porous graphene for enhanced oxygen reduction activity. Electrochim Acta. 2021;391:138956. https://doi.org/10.1016/j.electacta.2021.138956.
[112] Peng J, Tao P, Song C, Shang W, Deng T, Wu J. Structural evolution of Pt-based oxygen reduction reaction electrocatalysts. Chin J Catal. 2022;43(1):47. https://doi.org/10.1016/s1872-2067(21)63896-2.
[113] Kong F, Ren Z, Norouzi Banis M, Du L, Zhou X, Chen G, Zhang L, Li J, Wang S, Li M, Doyle-Davis K, Ma Y, Li R, Young A, Yang L, Markiewicz M, Tong Y, Yin G, Du C, Luo J, Sun X. Active and stable Pt-Ni alloy octahedra catalyst for oxygen reduction via near-surface atomical engineering. ACS Catal. 2020;10(7):4205. https://doi.org/10.1021/acscatal.9b05133.
[114] Xie M, Lyu Z, Chen R, Shen M, Cao Z, Xia Y. Pt-Co@Pt octahedral nanocrystals: enhancing their activity and durability toward oxygen reduction with an intermetallic core and an ultrathin shell. J Am Chem Soc. 2021;143(22):8509. https://doi.org/10.1021/jacs.1c04160.
[115] Zhao F, Zheng L, Yuan Q, Zhang Q, Sheng T, Yang X, Gu L, Wang X. PtCu subnanoclusters epitaxial on octahedral PtCu/Pt skin matrix as ultrahigh stable cathode electrocatalysts for room-temperature hydrogen fuel cells. Nano Res. 2022;16(2):2252. https://doi.org/10.1007/s12274022-5026-7.
[116] Zhu Y, Peng J, Zhu X, Bu L, Shao Q, Pao CW, Hu Z, Li Y, Wu J, Huang X. A large-scalable, surfactant-free, and ultrastable Ru-doped Pt_3Co oxygen reduction catalyst. Nano Lett. 2021;21(15):6625. https://doi.org/10.1021/acs.nanolett.1c02064.
[117] Polani S, MacArthur KE, Kang J, Klingenhof M, Wang X, Moller T, Amitrano R, Chattot R, Heggen M, Dunin-Borkowski RE, Strasser P. Highly active and stable large Mo-doped Pt-Ni octahedral catalysts for ORR: synthesis, post-treatments, and electrochemical performance and stability. ACS Appl Mater Interfaces. 2022;14(26):29690. https://doi.org/10.1021/acsami.2c02397.
[118] Xia T, Zhao K, Zhu Y, Bai X, Gao H, Wang Z, Gong Y, Feng M, Li S, Zheng Q, Wang S, Wang R, Guo H.

Mixed-dimensional Pt-Ni Alloy polyhedral nanochains as bifunctional electrocatalysts for direct methanol fuel cells. Adv Mater. 2023;35(2):2206508. https://doi.org/10.1002/adma.202206508.

[119] Wei M, Huang L, Li L, Ai F, Su J, Wang J. Coordinatively unsaturated PtCo flowers assembled with ultrathin nanosheets for enhanced oxygen reduction. ACS Catal. 2022;12(11):6478. https://doi.org/10.1021/acscatal.1c05153.

[120] Du X, Sun S, Ma G, Yu H, Wang M, Lu Z, Yu X, Li L, Zhang X, Yang X. Cu-template-dependent synthesis of PtCu nanotubes for oxygen reduction reactions. Int J Hydrogen Energy. 2022;47(9):6217. https://doi.org/10.1016/j.ijhydene.2021.11.215.

[121] Chen S, Li M, Gao M, Jin J, van Spronsen MA, Salmeron MB, Yang P. High-performance Pt-Co nanoframes for fuel-cell electrocatalysis. Nano Lett. 2020;20(3):1974. https://doi.org/10.1021/acs.nanolett.9b05251.

[122] Ma H, Zheng Z, Zhao H, Shen C, Chen H, Li H, Cao Z, Kuang Q, Lin H, Xie Z. Trimetallic PtNiCo branched nanocages as efficient and durable bifunctional electrocatalysts towards oxygen reduction and methanol oxidation reactions. J Mater Chem A. 2021;9(41):23444. https://doi.org/10.1039/d1ta07488a.

[123] Chen S, Zhao J, Su H, Li H, Wang H, Hu Z, Bao J, Zeng J. Pd-Pt tesseracts for the oxygen reduction reaction. J Am Chem Soc. 2021;143(1):496. https://doi.org/10.1021/jacs.0c12282.

[124] Zhang Y, Ye K, Liu Q, Qin J, Jiang Q, Yang B, Yin F. Ni^{2+}-directed anisotropic growth of PtCu nested skeleton cubes boosting electroreduction of oxygen. Adv Sci. 2022;9(14):2104927. https://doi.org/10.1002/advs.202104927.

[125] Zhu X, Huang L, Wei M, Tsiakaras P, Shen PK. Highly stable Pt-Co nanodendrite in nanoframe with Pt skin structured catalyst for oxygen reduction electrocatalysis. Appl Catal, B. 2021;281:119460. https://doi.org/10.1016/j.apcatb.2020.119460.

[126] Qin Y, Zhang W, Guo K, Liu X, Liu J, Liang X, Wang X, Gao D, Gan L, Zhu Y, Zhang Z, Hu W. Fine-tuning intrinsic strain in penta-twinned Pt-Cu-Mn nanoframes boosts oxygen reduction catalysis. Adv Funct Mater. 2020;30(11):1910107. https://doi.org/10.1002/adfm.201910107.

[127] Gong L, Liu J, Li Y, Wang X, Luo E, Jin Z, Ge J, Liu C, Xing W. An ultralow-loading platinum alloy efficient ORR electrocatalyst based on the surface-contracted hollow structure. Chem Eng J. 2022;428:131569. https://doi.org/10.1016/j.cej.2021.131569.

[128] Kang Y, Wang J, Wei Y, Wu Y, Xia D, Gan L. Engineering nanoporous and solid core-shell architectures of low-platinum alloy catalysts for high power density PEM fuel cells. Nano Res. 2022;15(7):6148. https://doi.org/10.1007/s12274-022-4238-1.

[129] Li S, Tang X, Jia H, Li H, Xie G, Liu X, Lin X, Qiu H-J. Nanoporous high-entropy alloys with low Pt loadings for high-performance electrochemical oxygen reduction. J Catal. 2020;383:164. https://doi.org/10.1016/j.jcat.2020.01.024.

[130] Yu T, Zhang Y, Hu Y, Hu K, Lin X, Xie G, Liu X, Reddy KM, Ito Y, Qiu H-J. Twelve-component free-standing nanoporous high-entropy alloys for multifunctional electrocatalysis. ACS Mater Lett. 2021;4(1):181. https://doi.org/10.1021/acsmaterialslett.1c00762.

[131] Huang L, Su YQ, Qi R, Dang D, Qin Y, Xi S, Zaman S, You B, Ding S, Xia BY. Boosting oxygen reduction via integrated construction and synergistic catalysis of porous platinum alloy and defective graphitic carbon. Angew Chem Int Ed Engl. 2021;60(48):25530. https://doi.org/10.1002/anie.202111426.

[132] Cheng H, Gui R, Yu H, Wang C, Liu S, Liu H, Zhou T, Zhang N, Zheng X, Chu W, Lin Y, Wu H, Wu C, Xie Y. Subsize Pt-based intermetallic compound enables long-term cyclic mass activity for fuel-cell oxygen reduction. Proc Natl Acad Sci U S A. 2021;118(35):2104026118. https://doi.org/10.1073/pnas.2104026118.

[133] Zhu S, Yang L, Bai J, Chu Y, Liu J, Jin Z, Liu C, Ge J, Xing W. Ultra-stable Pt_5La intermetallic compound towards highly efficient oxygen reduction reaction. Nano Res. 2022;16(2):2035. https://doi.org/10.1007/s12274-022-4868-3.

[134] Kim HY, Kwon T, Ha Y, Jun M, Baik H, Jeong HY, Kim H, Lee K, Joo SH. Intermetallic PtCu nanoframes as efficient oxygen reduction electrocatalysts. Nano Lett. 2020;20(10):7413. https://doi.org/10.1021/acs.nanolett.0c02812.

[135] Zhao W, Chi B, Liang L, Yang P, Zhang W, Ge X, Wang L, Cui Z, Liao S. Optimizing the electronic structure of ordered Pt-Co-Ti ternary intermetallic catalyst to boost acidic oxygen reduction. ACS Catal. 2022;12(13):7571. https://doi.org/10.1021/acscatal.2c00554.

[136] Gong M, Xiao D, Deng Z, Zhang R, Xia W, Zhao T, Liu X, Shen T, Hu Y, Lu Y, Zhao X, Xin H, Wang D. Structure evolution of PtCu nanoframes from disordered to ordered for the oxygen reduction reaction. Appl Catal, B. 2021;282:119617. https://doi.org/10.1016/j.apcatb.2020.119617.

[137] Bai J, Yang L, Jin Z, Ge J, Xing W. Advanced Pt-based intermetallic nanocrystals for the oxygen reduction reaction. Chin J Catal. 2022;43(6):1444. https://doi.org/10.1016/s1872-2067(21)63991-8.

[138] Yoo TY, Yoo JM, Sinha AK, Bootharaju MS, Jung E, Lee HS, Lee BH, Kim J, Antink WH, Kim YM, Lee J, Lee E, Lee DW, Cho SP, Yoo SJ, Sung YE, Hyeon T. Direct synthesis of intermetallic platinum-alloy nanoparticles highly loaded on carbon supports for efficient electrocatalysis. J Am Chem Soc. 2020;142(33):14190. https://doi.org/10.1021/jacs.0c05140.

[139] Ma Y, Kuhn AN, Gao W, Al-Zoubi T, Du H, Pan X, Yang H. Strong electrostatic adsorption approach to the synthesis of sub-three nanometer intermetallic platinum–cobalt oxygen reduction catalysts. Nano Energy. 2021;79:105465. https://doi.org/10.1016/j.nanoen.2020.105465.

[140] Luo Q, Xu W, Tang S. Fabricating high-loading ultra-small $PtCu_3$/rGO via a traceless protectant and spray-freeze-drying method. Appl Catal, B. 2022;312:121433. https://doi.org/10.1016/j.apcatb.2022.121433.

[141] Hu Y, Shen T, Zhao X, Zhang J, Lu Y, Shen J, Lu S, Tu Z, Xin HL, Wang D. Combining structurally ordered intermetallics with N-doped carbon confinement for efficient and anti-poisoning electrocatalysis. Appl Catal, B. 2020;279:119370. https://doi.org/10.1016/j.apcatb.2020.119370.

[142] Hu Y, Guo X, Shen T, Zhu Y, Wang D. Hollow porous carbon-confined atomically ordered $PtCo_3$ Intermetallics for an efficient oxygen reduction reaction. ACS Catal. 2022;12(9):5380. https://doi.org/10.1021/acscatal.2c01541.

[143] Yang CL, Wang LN, Yin P, Liu J, Chen MX, Yan QQ, Wang ZS, Xu SL, Chu SQ, Cui C, Ju H, Zhu J, Lin Y, Shui J, Liang HW. Sulfur-anchoring synthesis of platinum intermetallic nanoparticle catalysts for fuel cells. Science. 2021;374(6566):459. https://doi.org/10.1126/science.abj9980.

[144] Guo P, Xia Y, Liu B, Ma M, Shen L, Dai Y, Zhang Z, Zhao Z, Zhang Y, Zhao L, Wang Z. Low-loading Sub-3 nm PtCo nanoparticles supported on Co-N-C with dual effect for oxygen reduction reaction in proton exchange membrane fuel cells. ACS Appl Mater Interfaces. 2022;14(48):53819. https://doi.org/10.1021/acsami.2c15996.

[145] Yang Z, Yang H, Shang L, Zhang T. Ordered PtFeIr intermetallic nanowires prepared through a silica-protection strategy for the oxygen reduction reaction. Angew Chem Int Ed Engl. 2022;61(8):202113278. https://doi.org/10.1002/anie.202113278.

[146] Cheng Q, Yang S, Fu C, Zou L, Zou Z, Jiang Z, Zhang J, Yang H. High-loaded sub-6 nm Pt1Co1 intermetallic compounds with highly efficient performance expression in PEMFCs. Energy Environ Sci. 2022;15(1):278. https://doi.org/10.1039/d1ee02530a.
[147] Su J, Zhuang L, Zhang S, Liu Q, Zhang L, Hu G. Single atom catalyst for electrocatalysis. Chin Chem Lett. 2021;32(10):2947. https://doi.org/10.1016/j.cclet.2021.03.082.
[148] Han L, Cheng H, Liu W, Li H, Ou P, Lin R, Wang HT, Pao CW, Head AR, Wang CH, Tong X, Sun CJ, Pong WF, Luo J, Zheng JC, Xin HL. A single-atom library for guided monometallic and concentration-complex multimetallic designs. Nat Mater. 2022;21(6):681. https://doi.org/10.1038/s41563-022-01252-y.
[149] Yang Z, Xiang M, Zhu Y, Hui J, Jiang Y, Dong S, Yu C, Ou J, Qin H. Single-atom platinum or ruthenium on C_4N as 2D high-performance electrocatalysts for oxygen reduction reaction. Chem Eng J. 2021;42(6):131347. https://doi.org/10.1016/j.cej.2021.131347.
[150] Kim JH, Shin D, Lee J, Baek DS, Shin TJ, Kim YT, Jeong HY, Kwak JH, Kim H, Joo SH. A general strategy to atomically dispersed precious metal catalysts for unravelling their catalytic trends for oxygen reduction reaction. ACS Nano. 2020;14(2):1990. https://doi.org/10.1021/acsnano.9b08494.
[151] Li J, Banis MN, Ren Z, Adair KR, Doyle-Davis K, Meira DM, Finfrock YZ, Zhang L, Kong F, Sham TK, Li R, Luo J, Sun X. Unveiling the nature of Pt single-atom catalyst during electrocatalytic hydrogen evolution and oxygen reduction reactions. Small. 2021;17(11):20 07245.
[152] Wei ZX, Zhu YT, Liu JY, Zhang ZC, Hu WP, Xu H, Feng YZ, Ma JM. Recent advance in single-atom catalysis. Rare Met. 2021;40(4):767. https://doi.org/10.1007/s12598-020-01592-1.
[153] Chen JJ, Gu S, Hao R, Wang ZY, Li MQ, Li ZQ, Liu K, Liao KM, Wang ZQ, Huang H, Li YZ, Zhang KL, Lu ZG. Co single atoms and nanoparticles dispersed on N-doped carbon nanotube as high-performance catalysts for Zn-air batteries. Rare Met. 2022;41(6):2055. https://doi.org/10.1007/s12598-022-01974-7.
[154] Zhu X, Tan X, Wu KH, Haw SC, Pao CW, Su BJ, Jiang J, Smith SC, Chen JM, Amal R, Lu X. Intrinsic ORR activity enhancement of Pt atomic sites by engineering the d-band center via local coordination tuning. Angew Chem Int Ed Engl. 2021;60(40):21911. https://doi.org/10.1002/anie.202107790.
[155] Cheng X, Wang Y, Lu Y, Zheng L, Sun S, Li H, Chen G, Zhang J. Single-atom alloy with Pt-Co dual sites as an efficient electrocatalyst for oxygen reduction reaction. Appl Catal, B. 2022;306:121112. https://doi.org/10.1016/j.apcatb.2022.121112.
[156] Liu J, Bak J, Roh J, Lee KS, Cho A, Han JW, Cho E. Reconstructing the coordination environment of platinum single-atom active sites for boosting oxygen reduction reaction. ACS Catal. 2020;11(1):466. https://doi.org/10.1021/acscatal.0c03330.
[157] Liu B, Feng R, Busch M, Wang S, Wu H, Liu P, Gu J, Bahadoran A, Matsumura D, Tsuji T, Zhang D, Song F, Liu Q. Synergistic hybrid electrocatalysts of platinum alloy and single-atom platinum for an efficient and durable oxygen reduction reaction. ACS Nano. 2022;16(9):14121. https://doi.org/10.1021/acsnano.2c04077.
[158] Kan D, Lian R, Wang D, Zhang X, Xu J, Gao X, Yu Y, Chen G, Wei Y. Screening effective single-atom ORR and OER electrocatalysts from Pt decorated MXenes by first-principles calculations. J Mater Chem A. 2020;8(33):17065. https://doi.org/10.1039/d0ta04429f.
[159] Kan D, Wang D, Cheng Y, Lian R, Sun B, Chen K, Huo W, Wang Y, Chen G, Wei Y. Designing of efficient bifunctional ORR/OER Pt Single-atom catalysts based on O-terminated MXenes by first-principles calculations. ACS Appl Mater Interfaces. 2021;13(44):52508. https://doi.org/10.1021/acsami.1c12893.